Computer Simulation of Liquid Crystals

Prabal K. Maiti

Department of Physics

Indian Institute of Science, Bangalore

maiti@physics.iisc.ernet.in

http://www..physics.iisc.ernet.in/~maiti

Outline

Various kinds of liquid crystal:

- **Thermotropic**
- **Lyotropic**

- **Phase behavior of a special kind of thermotropic liquid crystal (Banana molecules and mixture of banana and rods)**
- **Self-assembly in surfactant solution (Lyotropic system)**
- **Self-assembly in chromonic liquid crystal (a special class of lyotropic system)**
- **Interfacial surface tension in liquid-crystal system (surfactant layer in between water and oil interface)**

What are liquid crystals?

isotropic

nematic

smectic A

smectic C

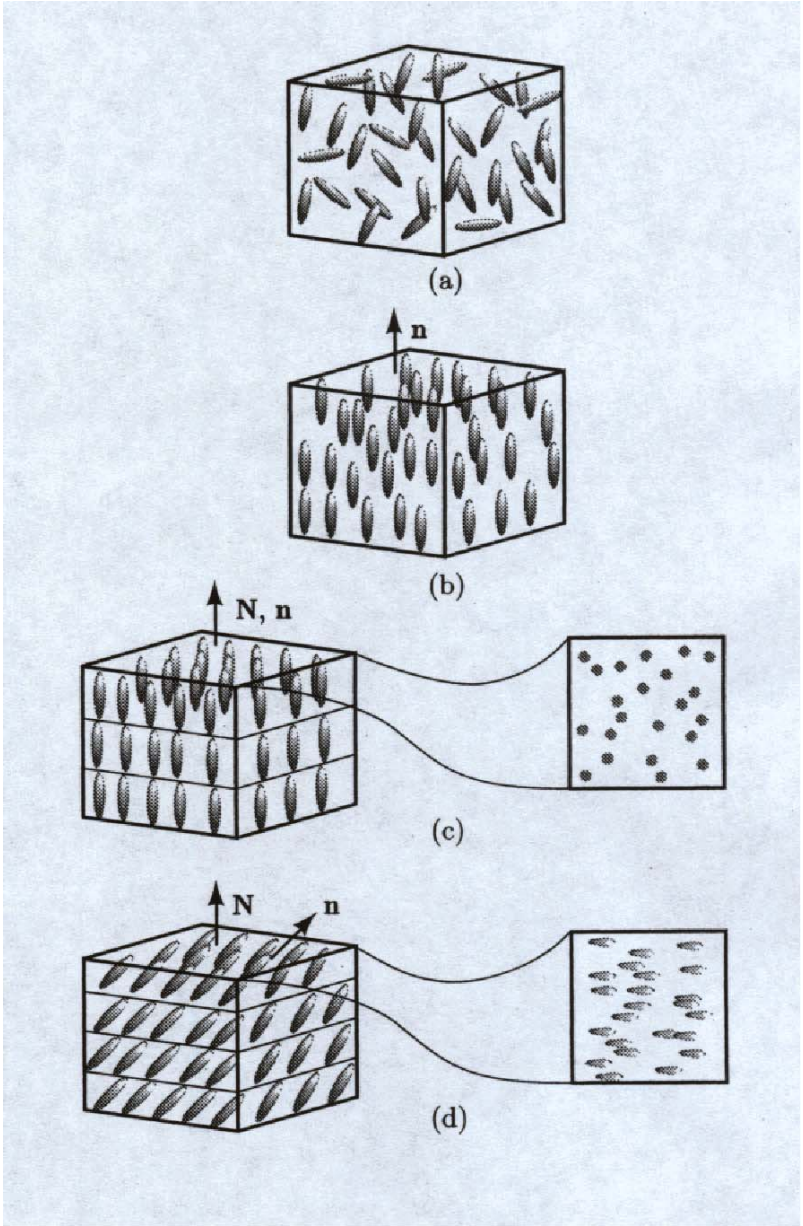

Phase changes as a function of temparature

Molecular orientational order (MOO)

MOO +
1d positional order

MOO +
1d positional order +
tilt order

Symmetry breaking with bent-core molecule

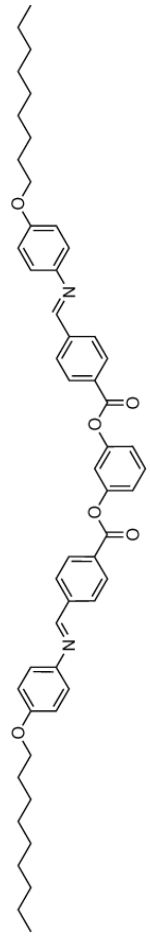

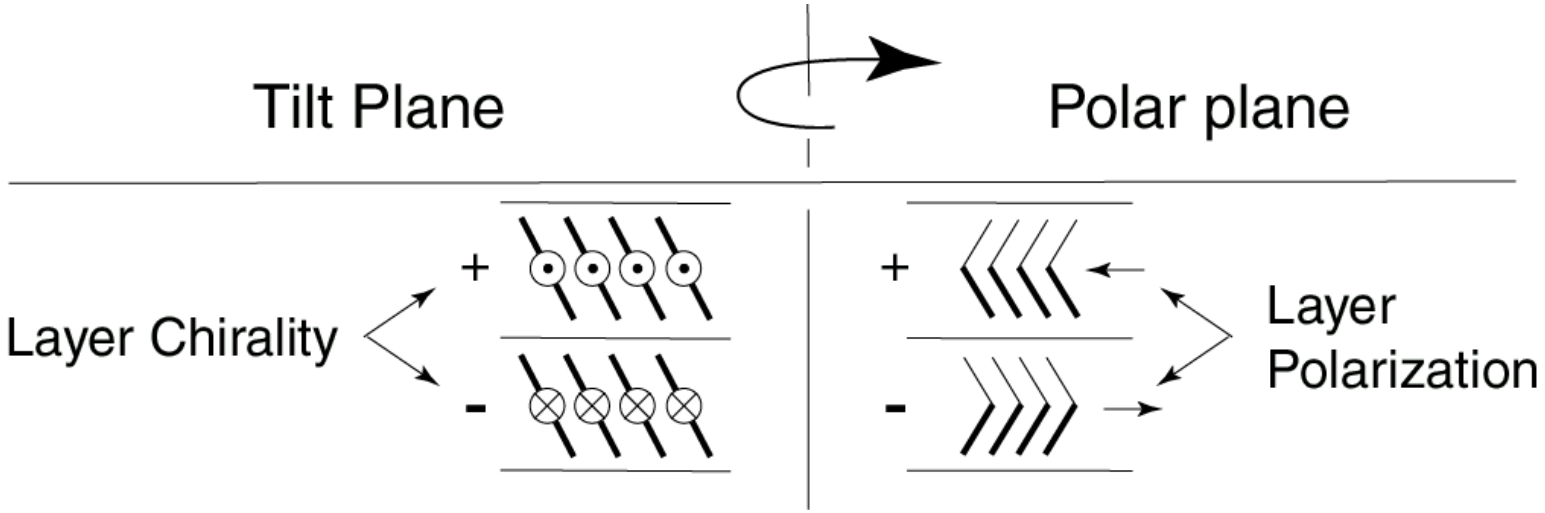

Spontaneous chiral symmetry breaking with achiral molecules

Motivation

molecular structure

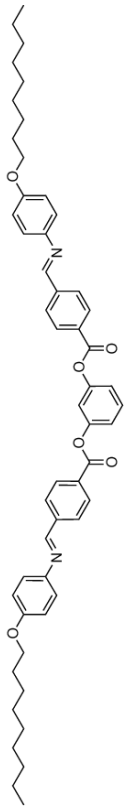

prediction

statistical mechanics

design

macroscopic properties

Hard-core spherocylinders

Phase transition driven only by entropic effects, at a given density:

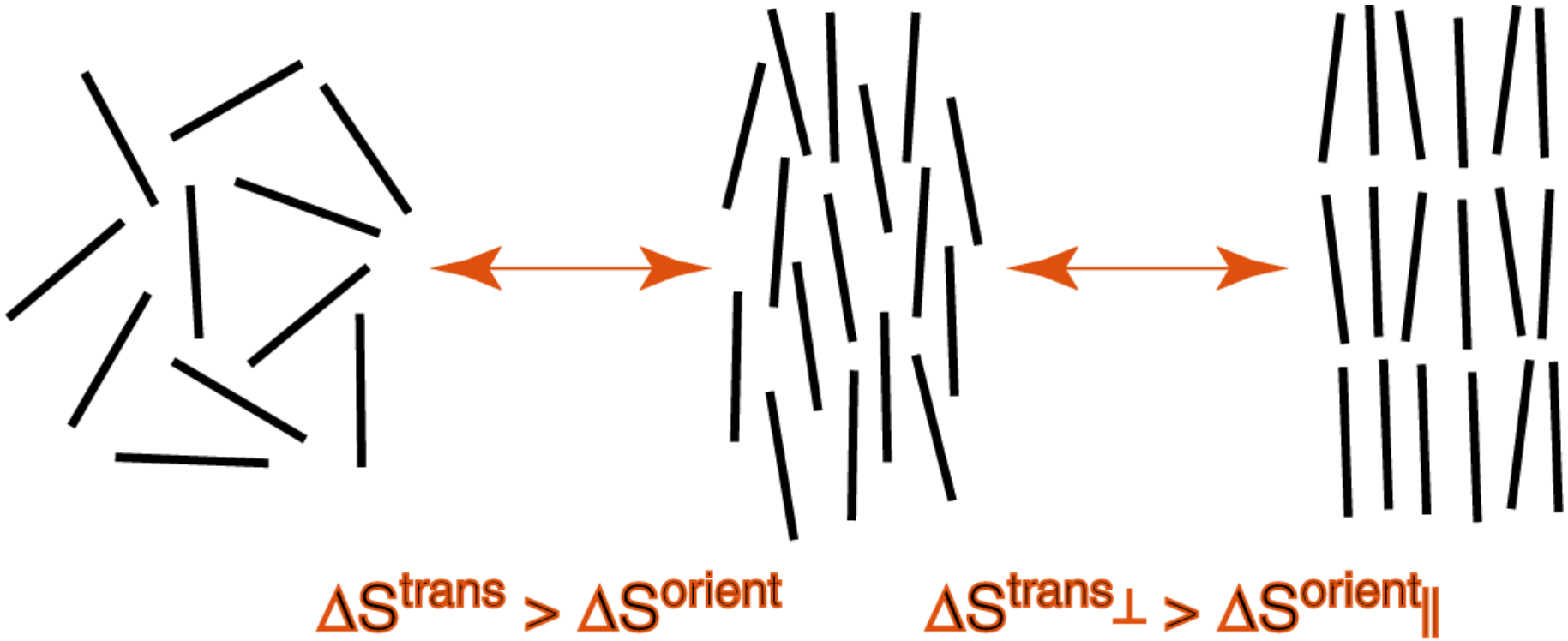

Outline

Achiral banana (bent-core) molecules exhibit spontaneous polar and chiral ordering

- What is the minimal molecular model that captures polar and/or chiral symmetry breaking?
- Are excluded volume interactions sufficient?

Very few materials exhibit both polar smectic and nematic phases

- What is the degree of molecular bending compatible with a nematic ordering?

The overwhelming majority of banana materials have an antiferroelectric ground state

- Is there some fundamental mechanism that favors antipolar ordering in banana phases?

A minimal model of rod/banana mixtures

We have studied mixtures of rod-shaped molecules (hard spherocylinders) and bow-shaped molecules (hard spherocylinder dimers) via Monte Carlo simulation

This model enables us to investigate the role of excluded volume (entropic) effects in rod/banana mixtures

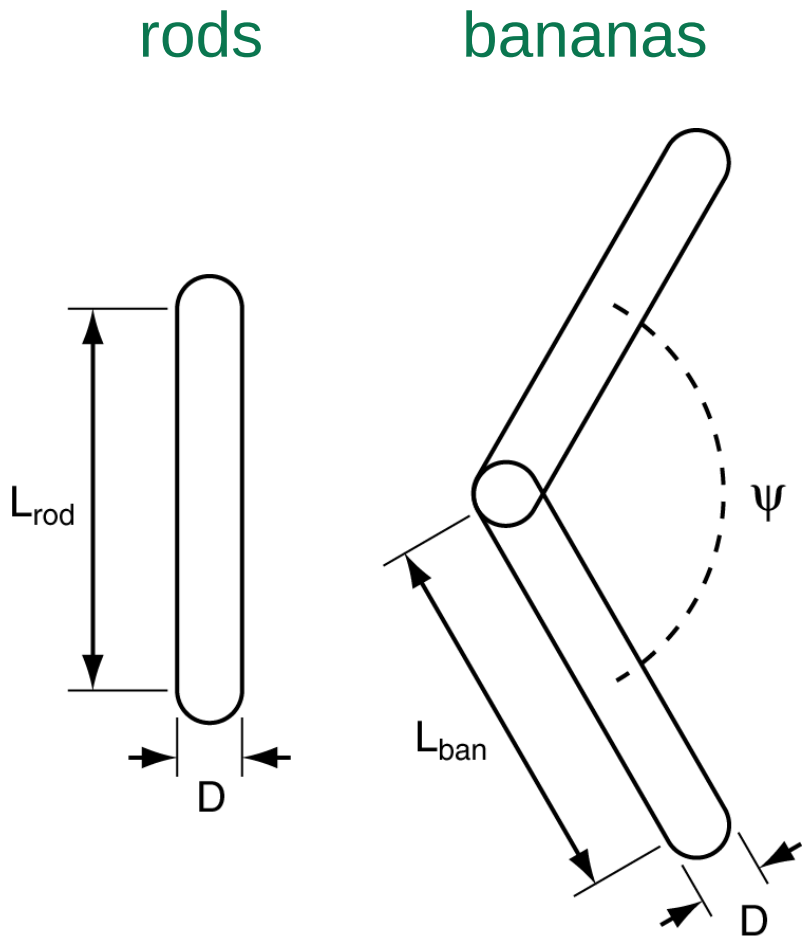

Rigid body Monte Carlo

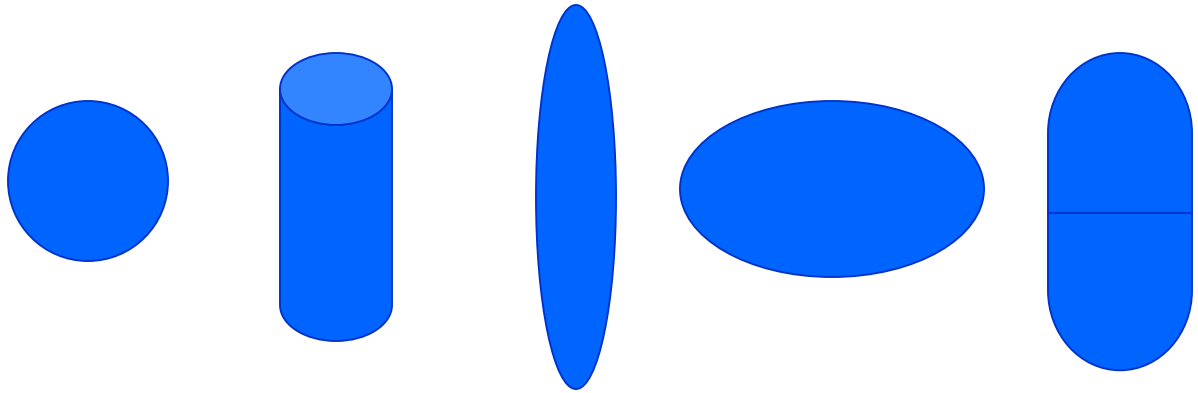

Sphere Cylinder Prolate ellipsoid disk spherocylinder

Each MC moves consists of translation and rotation of molecules. Rotation is performed through Quaternion.

Move is accepted with Boltzmann criteria if there is no overlap

Whole exercise is to devise efficient algorithm to do the overlap check

Quaternion dynamics

The quaternion are related to the Euler angles as follows:

$$q_o = \cos\frac{\theta}{2}\cos(\phi+\psi)/2$$

$$q_1 = \sin\frac{\theta}{2}\cos(\phi+\psi)/2$$

$$q_2 = \sin\frac{\theta}{2}\sin(\phi+\psi)/2$$

$$q_3 = \cos\frac{\theta}{2}\sin(\phi+\psi)/2$$

The quaternion satisfy the constraint

$$q_0^2 + q_1^2 + q_2^2 + q_3^2 = 1$$

The Euler angle rotation matrix can be written as

$$\begin{pmatrix} q_0^2+q_1^2-q_2^2-q_3^2 & 2\left(q_1q_2+q_0q_3\right) & 2\left(q_1q_3-q_0q_2\right) \\ 2\left(q_1q_2-q_0q_3\right) & q_0^2-q_1^2+q_2^2-q_3^2 & 2\left(q_2q_3+q_0q_1\right) \\ 2\left(q_1q_3-q_0q_2\right) & 2\left(q_2q_3-q_0q_1\right) & q_0^2-q_1^2-q_2^2+q_3^2 \end{pmatrix}$$

Overlap test for sphere

Two hard spheres of radius R_1 and R_2 overlap if the distance between the center of the two spheres r_{12} is less than $\sigma_{12} = R_1 + R_2$

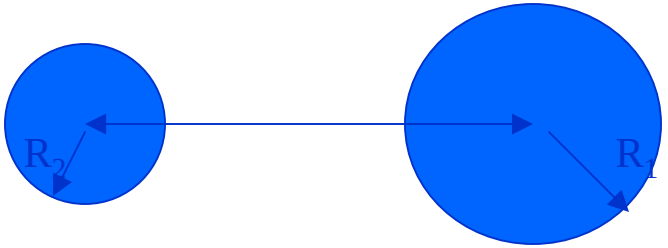

In simulation we do not compare r_{12} with σ_{12} but r^2_{12} with σ^2_{12}. Later test is cheaper computationally.

In general above test can be decomposed into sequence of several smaller test. In this case the steps are

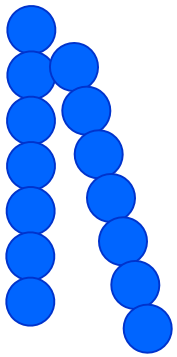

What happens if we have molecules composed of n hard spheres : In this case the overlap between two molecules can be broken down into n2 hard sphere tests

Ref: Hard convex body fluids, M. P. Allen et. al Advances in Chemical Physics, Volume LXXXVI, 1-165 (1993) (edited by I Prigogine and S. A. Rice)

Overlap test for spherocylinders

Just as a sphere can be defined as the set of points that are within a distance *R* from a given origin (center of sphere). The spherocylinder can be thought of as set of points that are within a distance *R* from a line segment of length *L*. We can draw around every point on this line segment a sphere of radius *R* that contains all points that are within a distance *R* from that point.

So a spherocylinder can be considered as the union of all spheres around points on a line segment L The test for the overlap between two spherocylinders can be done by computing the shortest distance between two line segments that from the core of the spherocylinders. If this distance of closest approach is less than $D_{12} = R_1 + R_2$, the two spherocylinders overlap.

Main task is to determine the distance of closest approach for the two line

We want to determine the minimum distance between two finite line segments i and j with orientations $\hat{\mathbf{u}}_i$ and $\hat{\mathbf{u}}_j$ and centers r_i and r_j. We can describe any point on line i parametrically as

$$r_i(\lambda) = r_i + \lambda \hat{u}_i$$

Line j is given by

$$r_j(\mu) = r_j + \mu \hat{u}_j$$

The vector distance between these two points is given by

$$r_{ij}(\lambda, \mu) = (r_i - r_j) + \lambda \hat{u}_i - \mu \hat{u}_j$$

Now we want to determine the values of λ and μ for which the distance r_{ij} is minimum. A simple method to find these values of λ and μ is the following. Construct the dot product of r_{ij} with $\hat{u}_i$ and $\hat{u}_j$. The shortest distance vector must be perpendicular to both $\hat{u}_i$ and $\hat{u}_j$

Our task is to solve the following equations

$$\left(r_i - r_j\right) \cdot \hat{u}_i = -\lambda \hat{u}_i \cdot \hat{u}_j + \mu \hat{u}_j \cdot \hat{u}_i$$

$$\left(r_i - r_j\right) \cdot \hat{u}_j = -\lambda \hat{u}_i \cdot \hat{u}_j + \mu \hat{u}_j \cdot \hat{u}_i$$

Solving for λ and μ we have

$$\begin{pmatrix}\lambda_0\\ \mu_0\end{pmatrix}=\frac{1}{1-\left(\hat{u}_i\cdot\hat{u}_j\right)^2}\begin{pmatrix}-\hat{u}_i\cdot r_{ij}+\left(\hat{u}_i\cdot\hat{u}_j\right)\left(\hat{u}_j\cdot r_{ij}\right)\\ +\hat{u}_j\cdot r_{ij}-\left(\hat{u}_i\cdot\hat{u}_j\right)\left(\hat{u}_i\cdot r_{ij}\right)\end{pmatrix}$$

If the spherocylinders are parallel

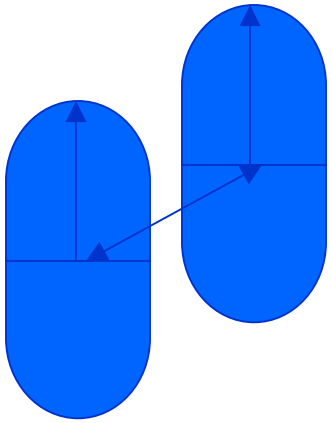

$$r_{ij}\cdot\hat{u}_i=r_{ij}\cdot\hat{u}_j$$

$$\left(\lambda_0\right)=\frac{1}{1-\left(\hat{u}_i\cdot\hat{u}_j\right)^2}\left(-\hat{u}_i\cdot r_{ij}+\left(\hat{u}_i\cdot\hat{u}_j\right)\left(\hat{u}_j\cdot r_{ij}\right)\right)$$

$$=\frac{-\hat{u}_i\cdot r_{ij}\left(1-\hat{u}_i\cdot\hat{u}_j\right)}{\left(1+\hat{u}_i\cdot\hat{u}_j\right)\left(1-\hat{u}_i\cdot\hat{u}_j\right)}=\frac{-\hat{u}_i\cdot r_{ij}}{2}$$

$$\mu_0=\frac{\hat{u}_j\cdot r_{ij}}{2}$$

If the spherocylinders are perpendicular

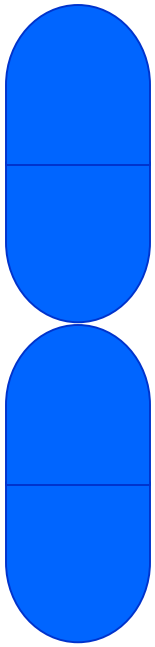

$$z_{ij} = \frac{L_i}{2} + \frac{L_j}{2} + D$$

Phase diagram of the hard spherocylinder system

P. Bolhuis and D. Frenkel, *J. Chem. Phys.* **106**, 666 (1997); S. C. McGrother, D. C. Williamson, and G. Jackson, *J. Chem. Phys.* **104**, 6755 (1996)

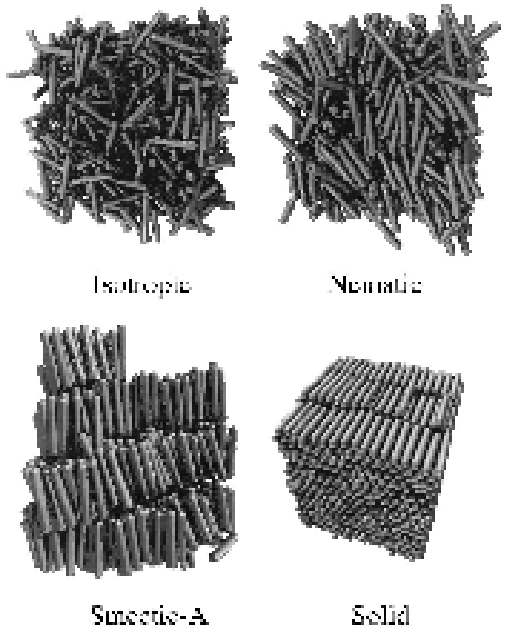

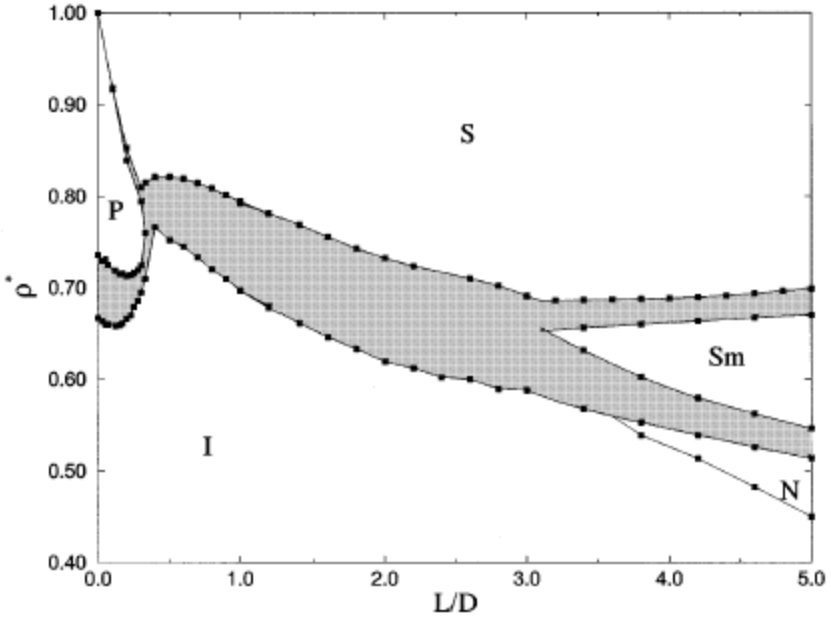

The thermodynamic properties of the hard spherocylinder system depend on the length to breadth ratio L / D and the reduced density $\rho^* = \rho\, v_0$, where ρ is the molecular number density and v_0 is the spherocylinder volume

Model

Hard spherocylinder dimers

Three-parameter model:

length / breadth ratio: L / D

opening angle: Ψ

reduced density or pressure: $\rho^* = \rho\, v_0$
or $P^* = \beta\, P\, v_0$

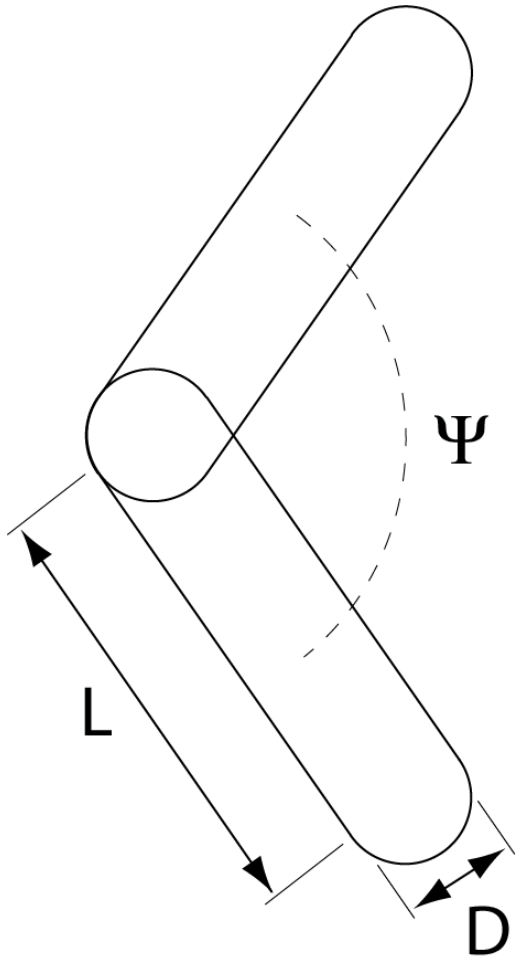

We study the phase diagram as a function of pressure and opening angle for **L / D = 5** by NPT Monte Carlo simulation

Phase diagram for L / D = 5

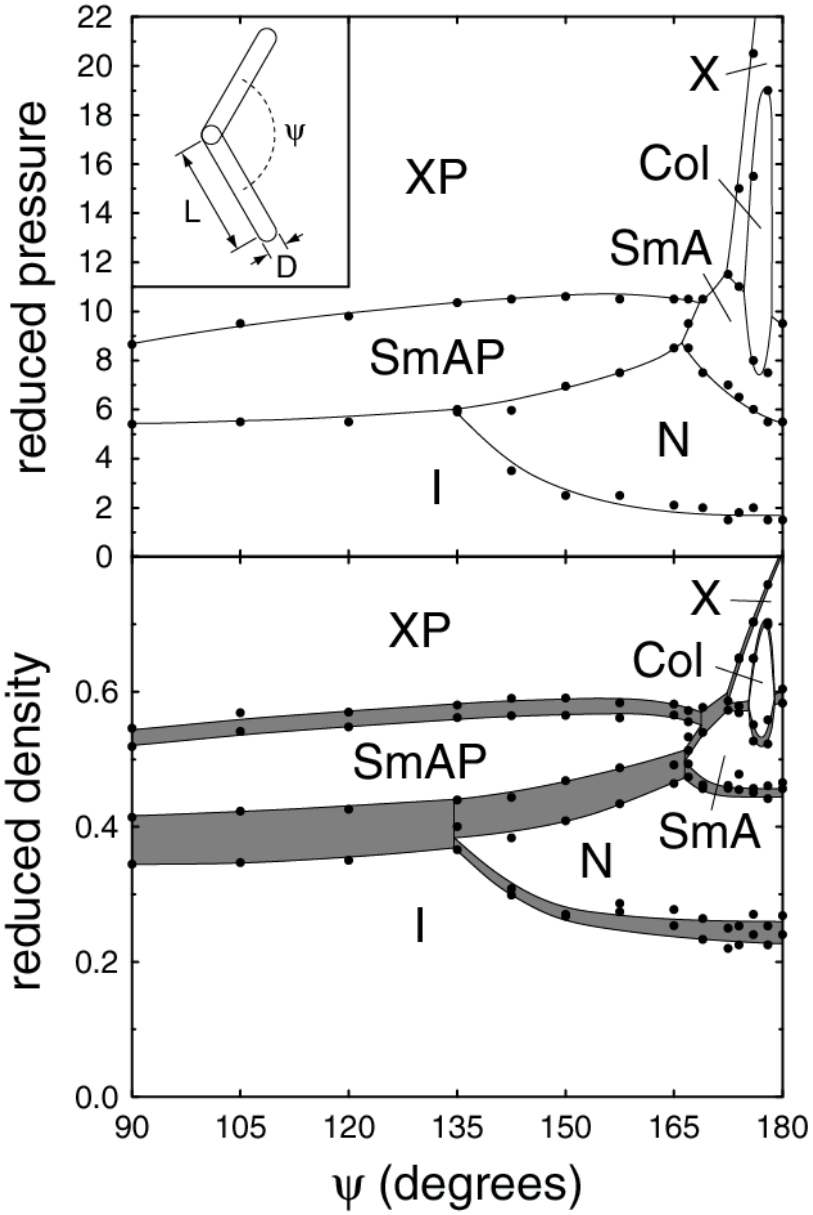

***Isotropic fluid* (I)**
***Nematic* (N)**
***Polar smectic A* (SmAP)**
***Smectic A* (SmA)**
***Columnar* (Col)**
***Polar crystal* (XP)**
***Crystal* (X)**

No chiral (tilted) smectic phase found.

PRE 67, 011703 (2003)

Final configurations for $\Psi = 90^{o}$

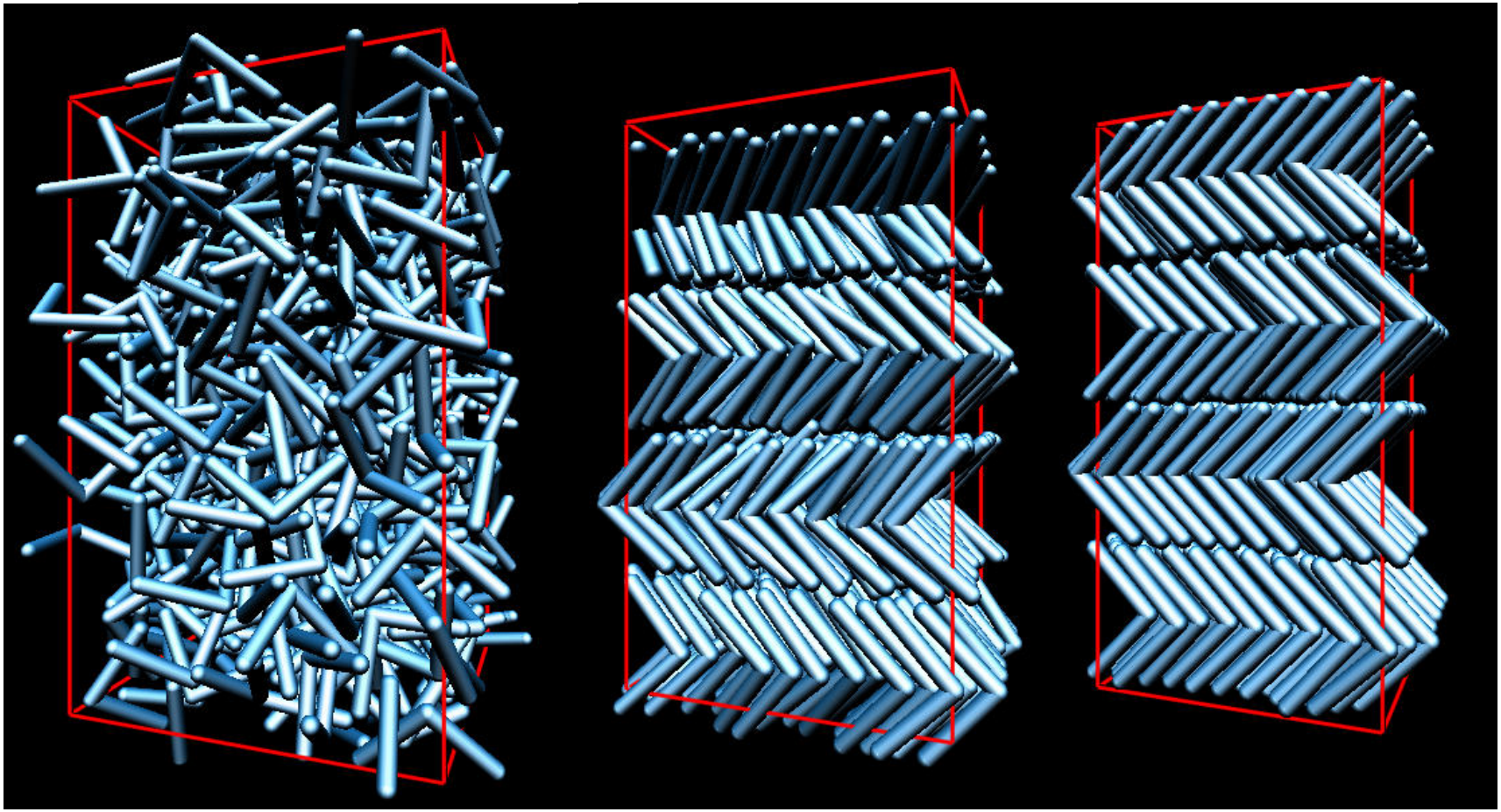

Isotropic
P* = 1

SmAP
P* = 7

Crystal
P* = 15

Final configurations for $\Psi = 165^{o}$

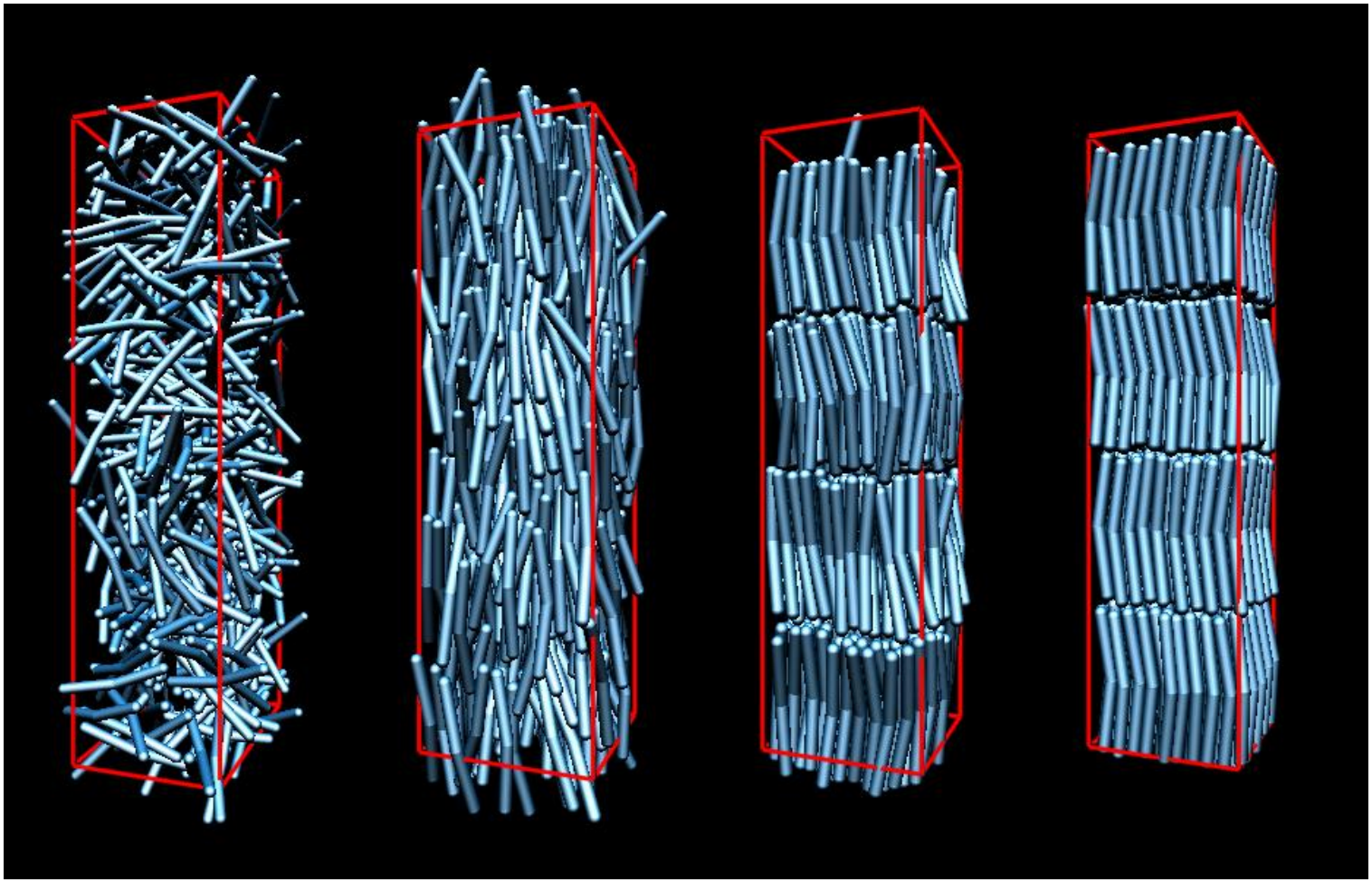

Isotropic	*Nematic*	*SmAP*	*Crystal*
P* = 1	P* = 5	P* = 9	P* = 15

Polar and nonpolar smectic A phases

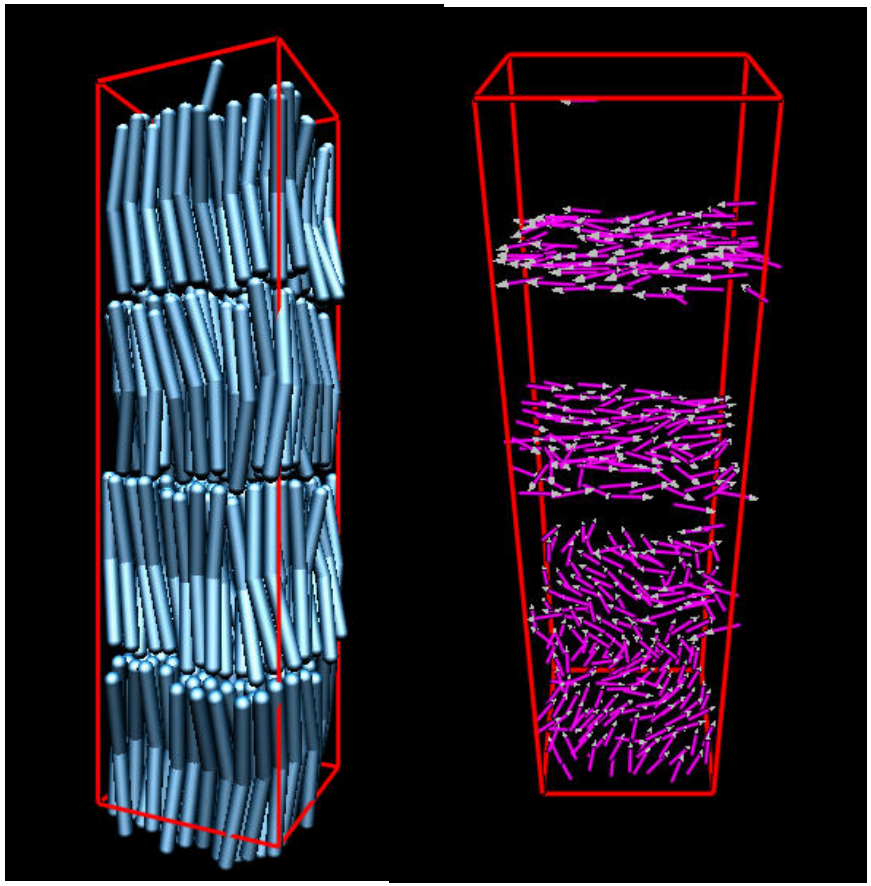

SmAP (in-layer polarity)
Ψ = 165°

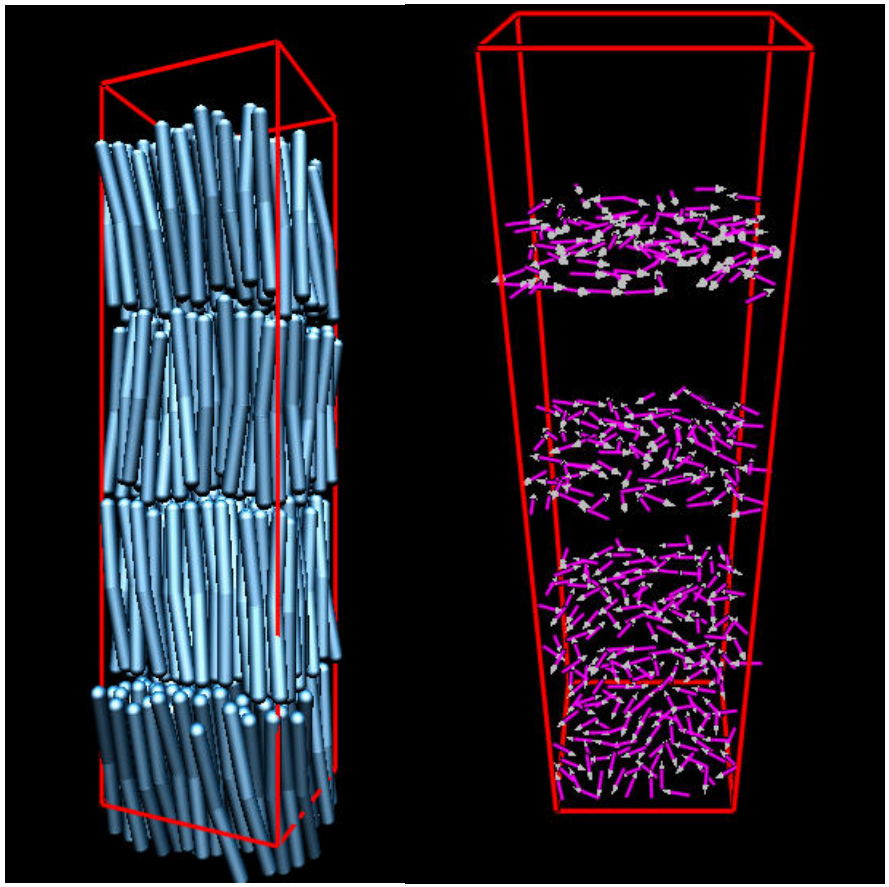

SmA (no polarity)
Ψ = 172.5°

Nature of the SmAP phase

Free energy calculation using umbrella sampling
$\Psi = 120^o$ at P = 7.5 (middle of the SmAP phase)*

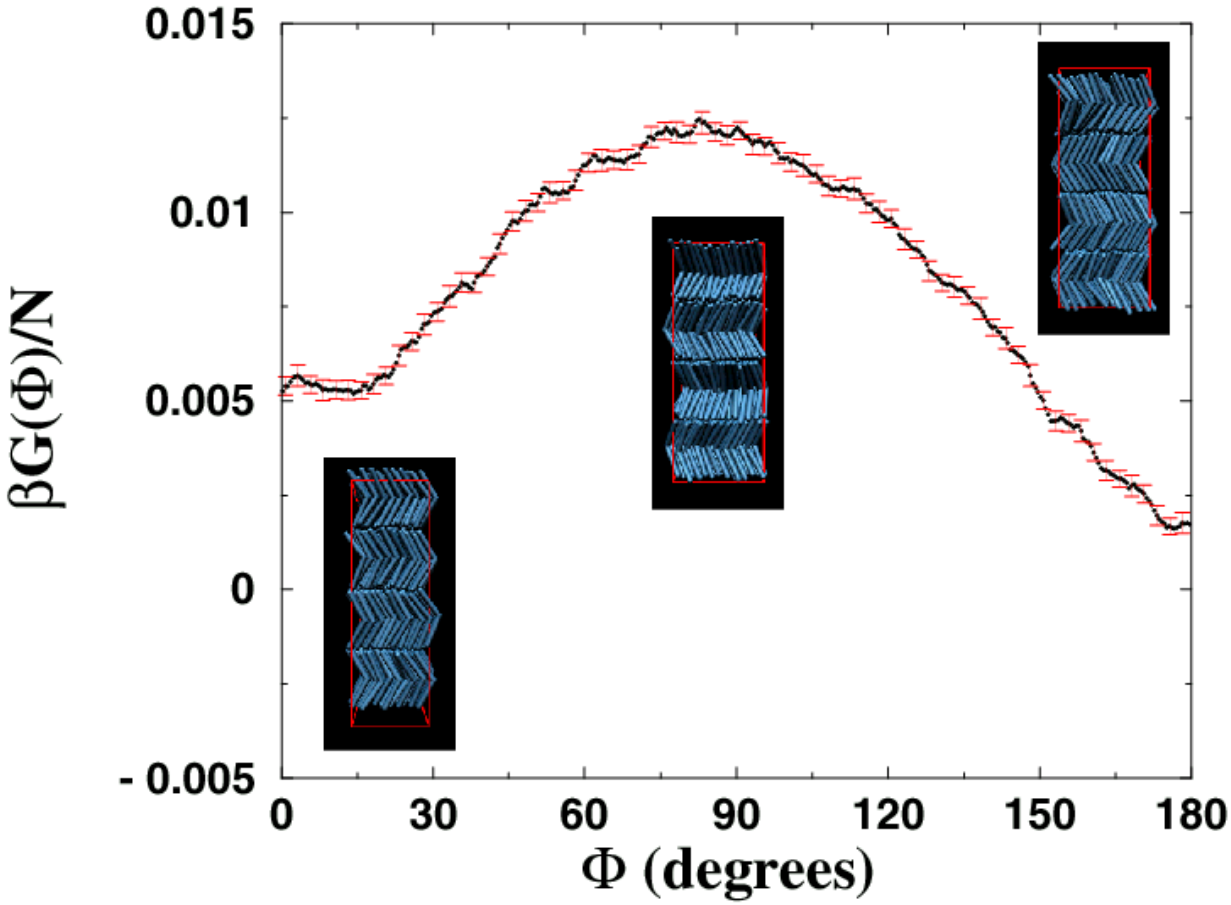

Entropic effects stabilize the antipolar SmAP phase

Sawtooth Model

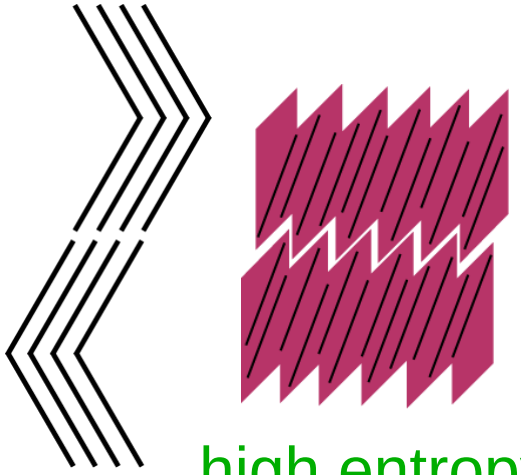

high entropy

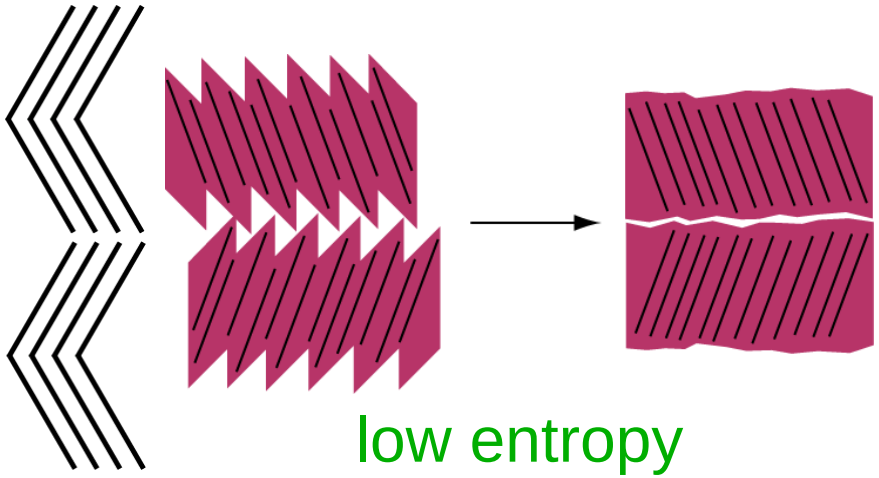

low entropy

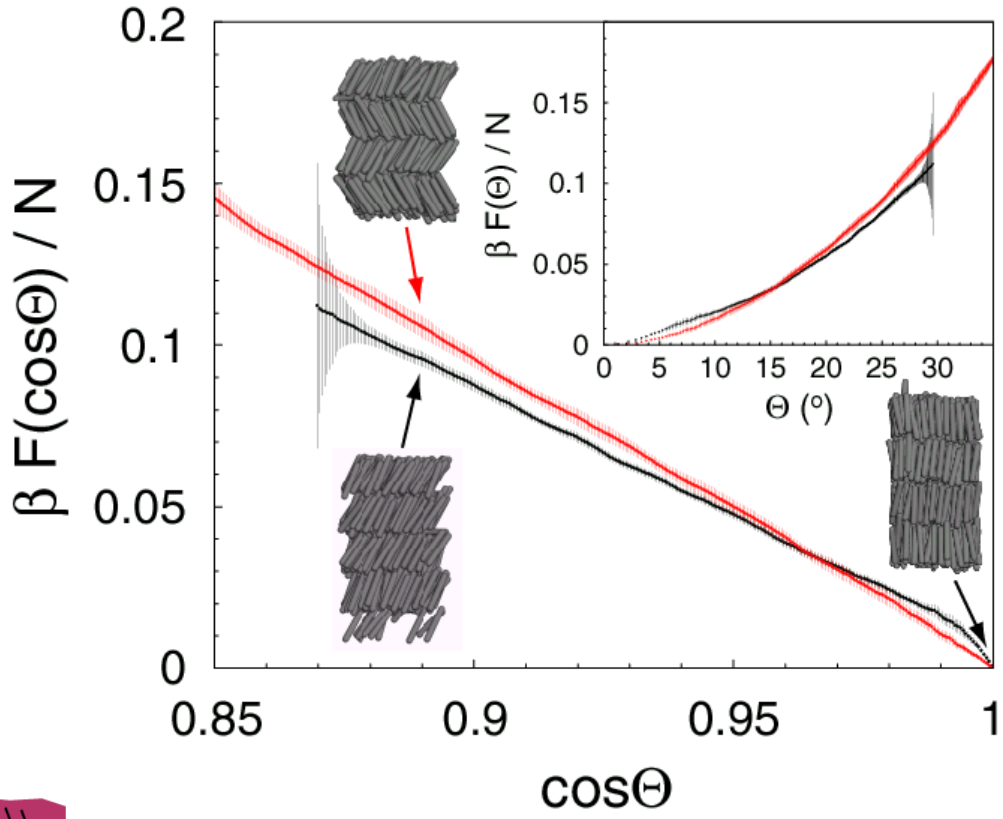

Liquid Crystals are Exotic Solvents

- Nematics impose orientational order on non-spherical solutes
- Smectics impose one-dimensional positional order (as well as orientational order) on solutes
  - **Organic lyotropics (T.P. Rieker, Liquid Crystals 19, 197 (1995))**
  - **Enhancement of polymerization rate (C.A. Guymon et al., Science 275, 57 (1997))**
- Smectic C solvents impose polar orientational order on low-symmetry solutes
  - **Chiral solutes contribute to ferroelectric polarization**

nanophase segregation in a smectic solvent

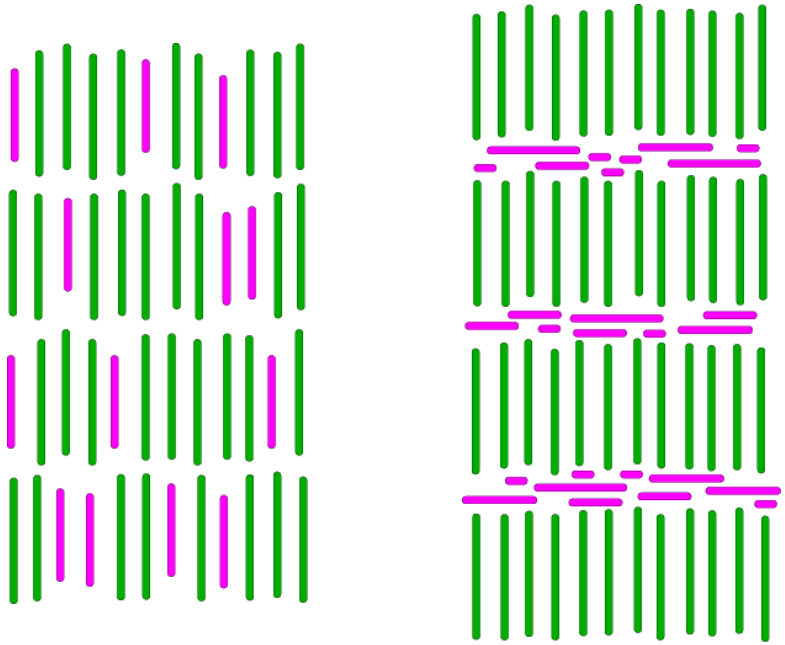

intralamellar segregation

interlamellar segregation

An orientational transition of bent-core molecules in an anisotropic matrix

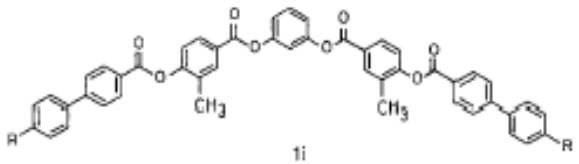

1i

R = C_nH_{2n+1}, n = 4 (1a), 5 (1b) 12 (1i)

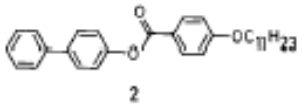

2

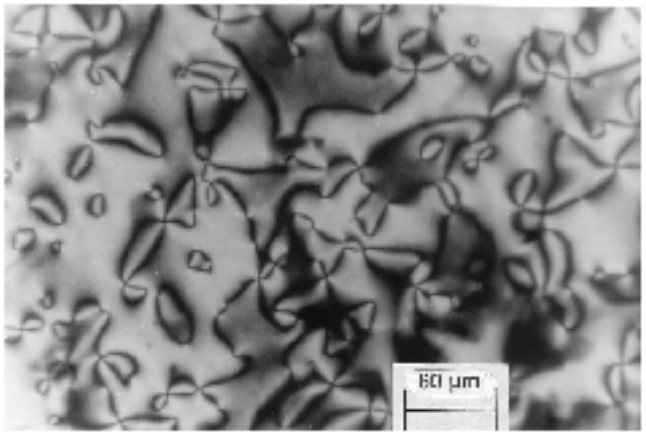

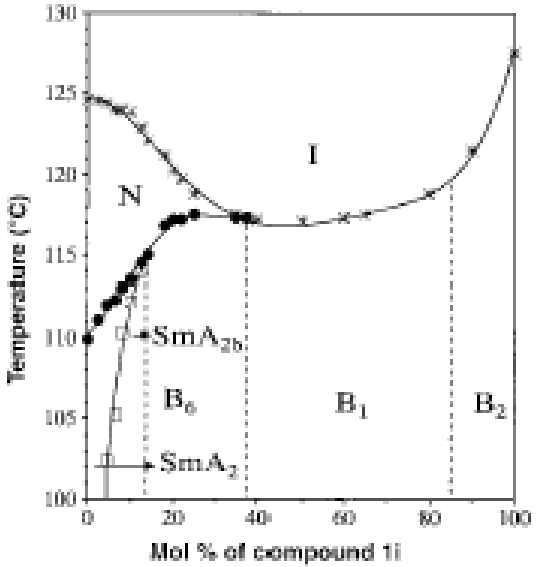

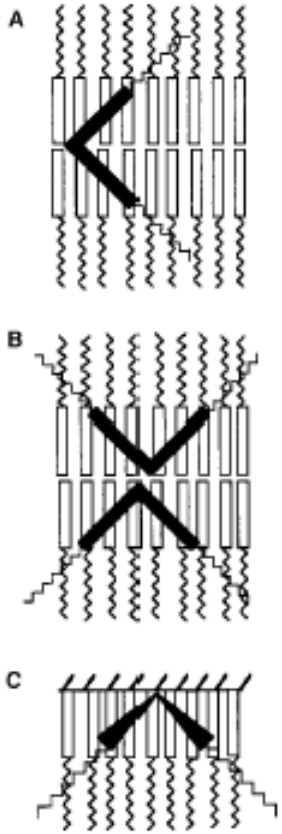

R. Pratibha, N. V. Madhusudana, B. K. Sadashiva, Science 288, 2184 (2000)

Induced anticlinic ordering for L_{ban} / D = 5 and c_{ban} = 3%

Anticlinic (SmC_A) ordering is induced for intermediate opening angles

For small opening angles, the system exhibits SmA ordering, with half of each banana molecule intercalated between smectic layers

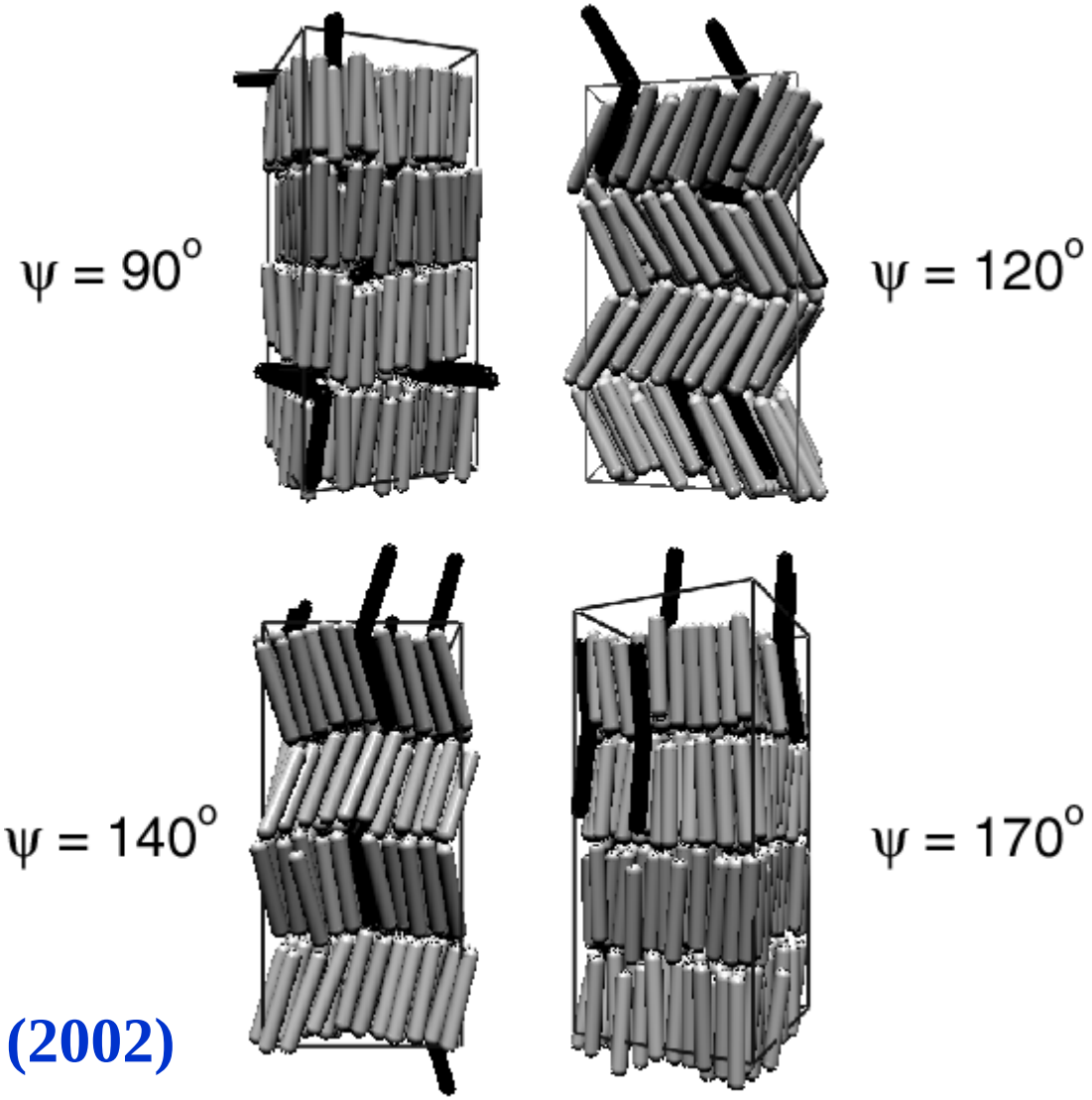

PRL, 88, 065504 (2002)

Sergeants and Soldiers

- A low concentration of longer bow-shaped molecules can induce anticlinic ordering

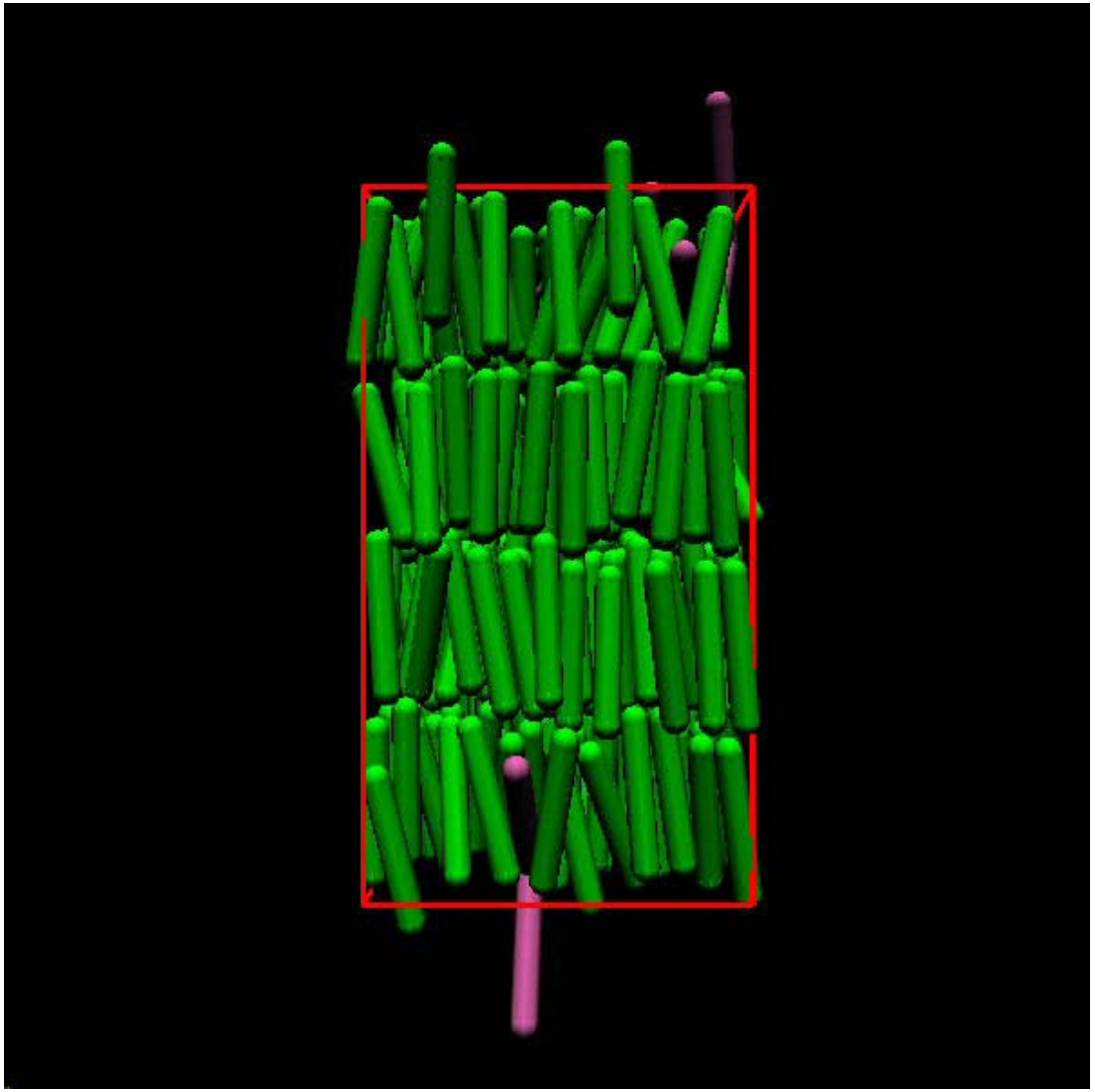

Induced anticlinic ordering for $L_{ban} / D = 5$ and $c_{ban} = 3\%$

Anticlinic ordering is observed for $100^o \leq \psi < 150^o$

The anticlinic tilt angle approximately shows the 'ideal' dependence $\theta = (\pi - \psi) / 2$ over this range

Molecular tilt leads to a decrease in layer spacing over this range

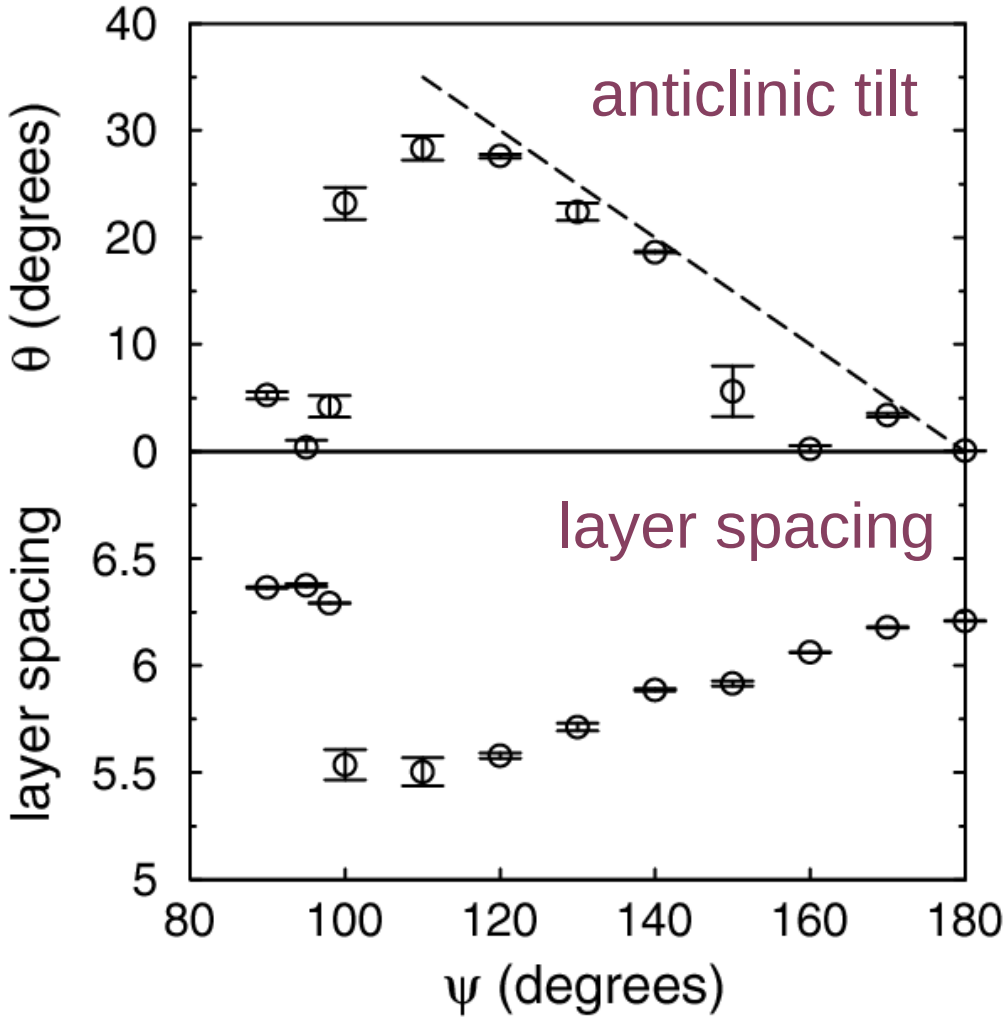

Free energy vs. tilt angle in the hard spherocylinder system

The entropic cost of a 30^{o} tilt in the hard spherocylinder system is modest (~ 0.1 $k_B T$ / molecule)

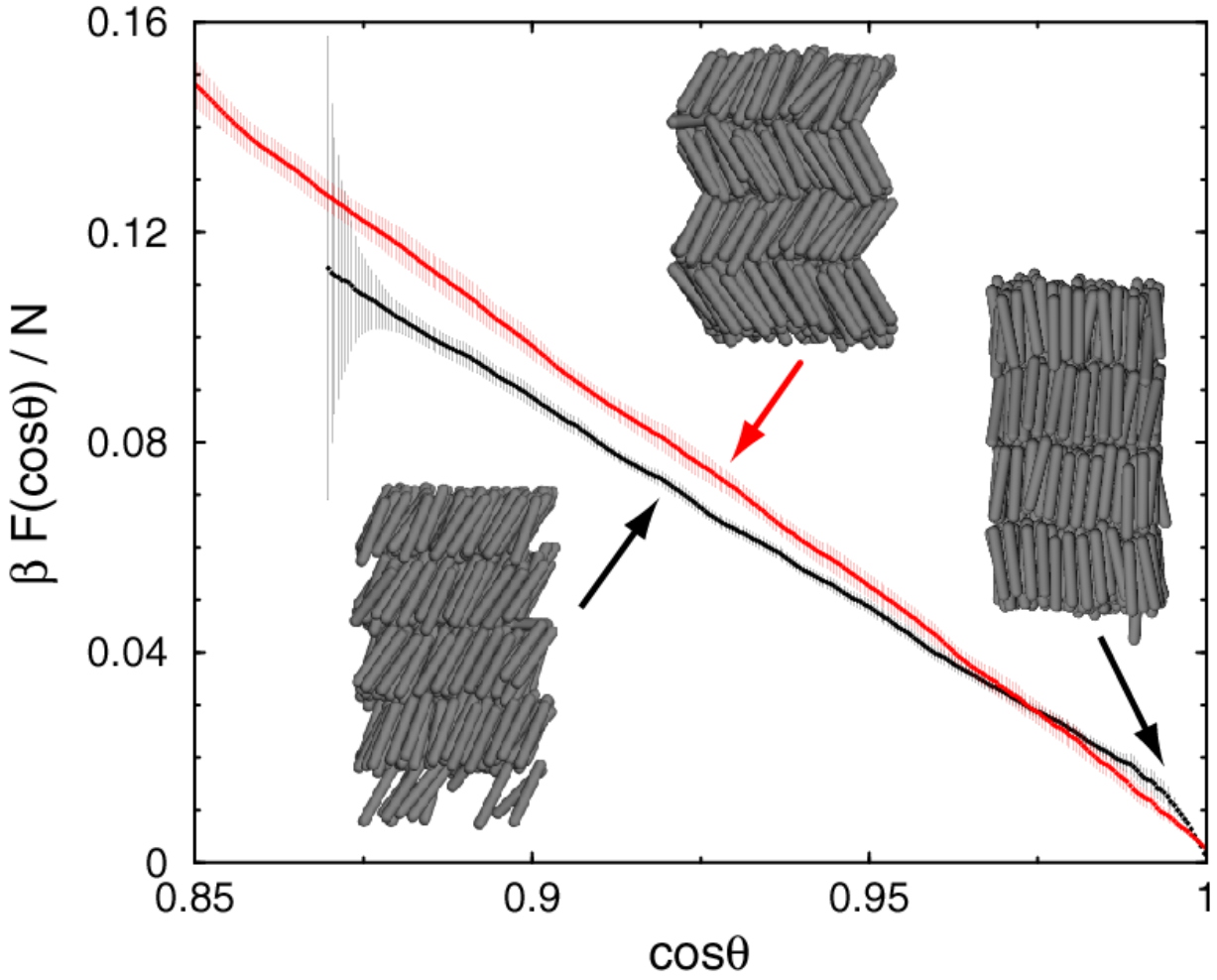

Estimated transition point

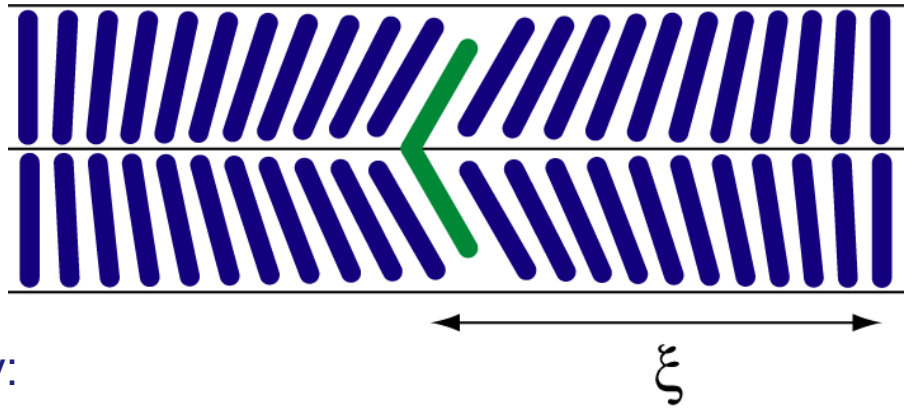

free energy density:

$$f = \tfrac{1}{2} K (\nabla\theta)^2 + \tfrac{1}{2} a \theta^2$$

decay length:

$$\xi = (K / a)^{1/2}$$

hard ellipsoids, dense nematic phase (B. Tjipto-Margo et al., JPC 96, 3942 (1992))

$$K \sim 1 - 10\, k_B T / D$$

hard spherocylinders, SmA phase (M. A. Glaser and N. A. Clark, unpublished)

$$a \sim 0.1\, k_B T / D^3$$

this gives

$$\xi \sim 10\, D$$

we expect a transition to the SmCA phase for $\rho_{ban} \sim 1 / (d\, \xi^2)$, or

$$c_{ban} \sim 0.01$$

Intralamellar-interlamellar transition for L_{ban} / D = 2.5 and c_{ban} = 3%

For large opening angles, banana molecules are segregated within smectic layers

For small opening angles, banana molecules are segregated between smectic layers

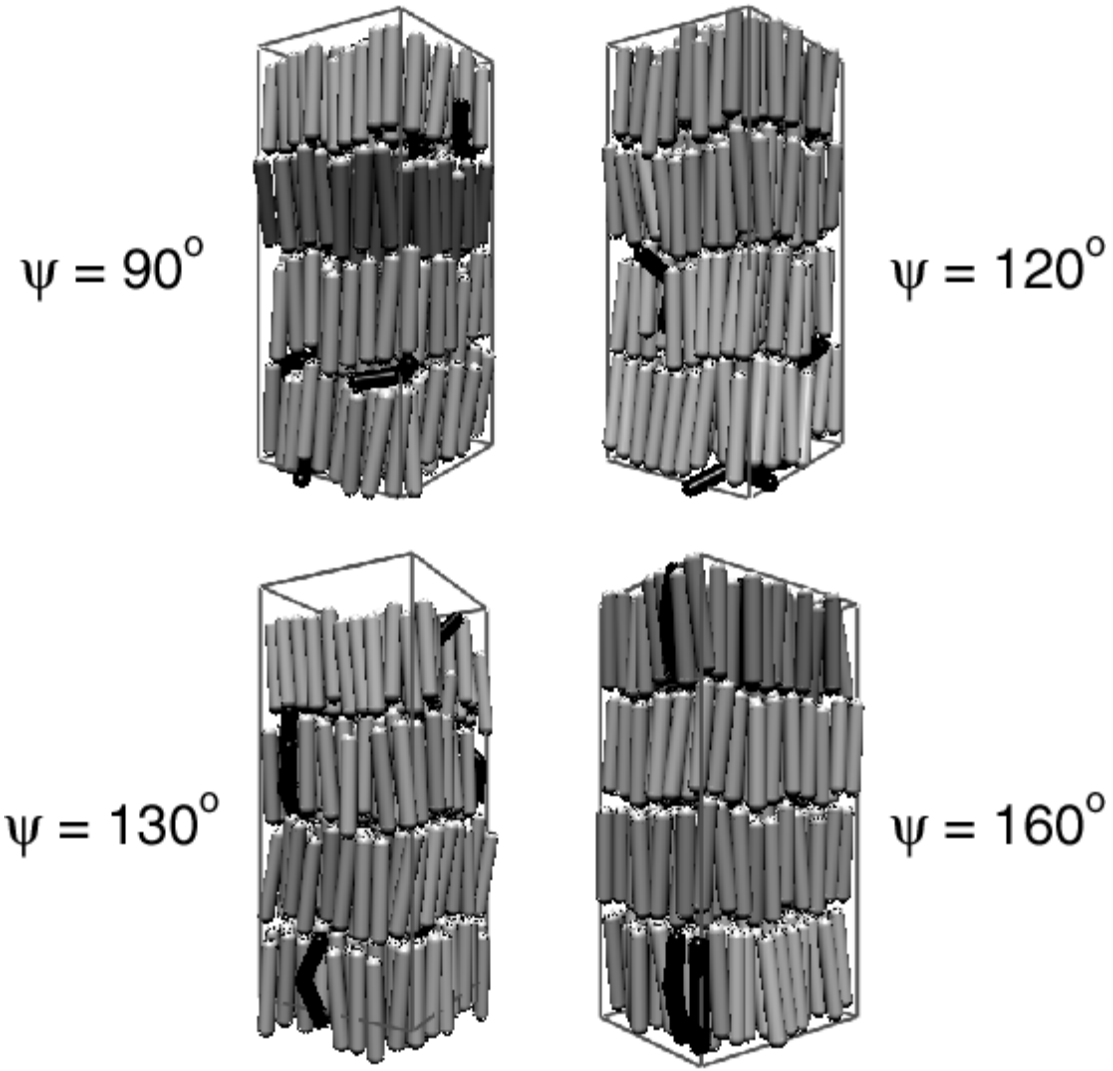

Nanophase segregation in rod/banana mixtures

- Monte Carlo simulations of mixtures of hard spherocylinders and hard bananas (spherocylinder dimers)
- Excluded volume interactions can produce nanophase segregation of bow-shaped molecules
- In other words, nanophase segregation can be entropy-driven

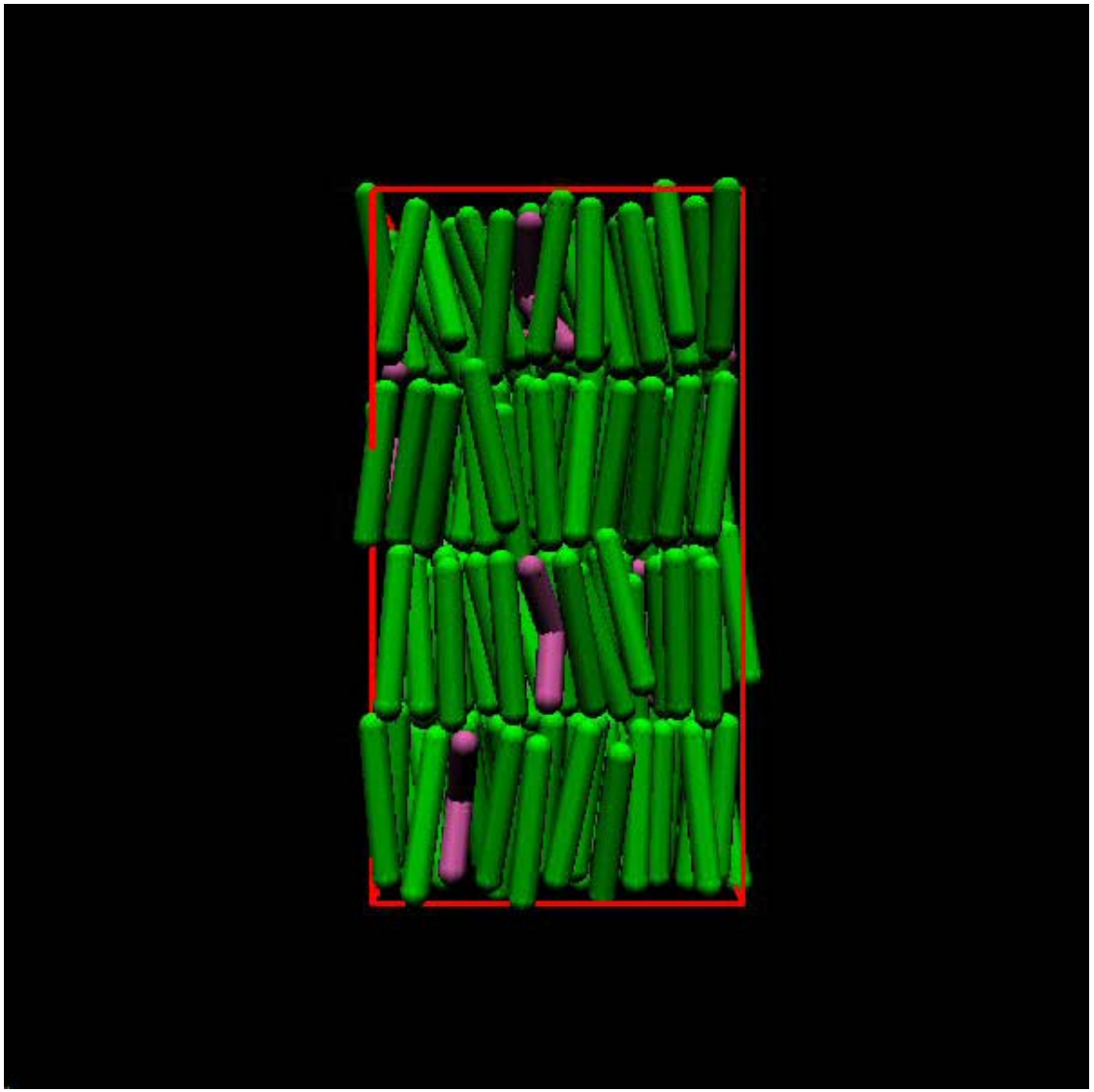

Number density profiles for L_{ban} / D = 2.5

rods

bananas

A transition from intralamellar to interlamellar nanophase segregation is observed near $\psi = 130^{o}$

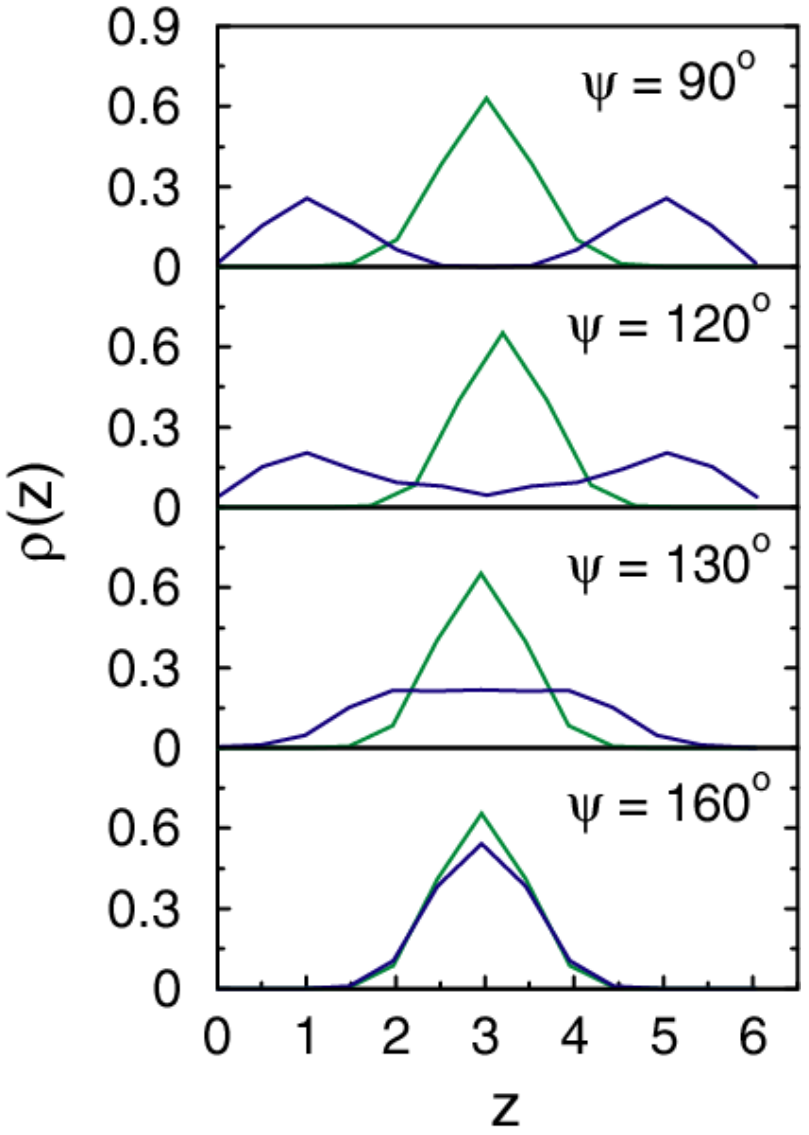

Intralamellar-interlamellar transition for L_{ban} / D = 2.5 and c_{ban} = 3%

No anticlinic ordering is observed

A sharp transition from *intralamellar* to *interlamellar* nanophase segregation occurs near $\psi = 130^{o}$

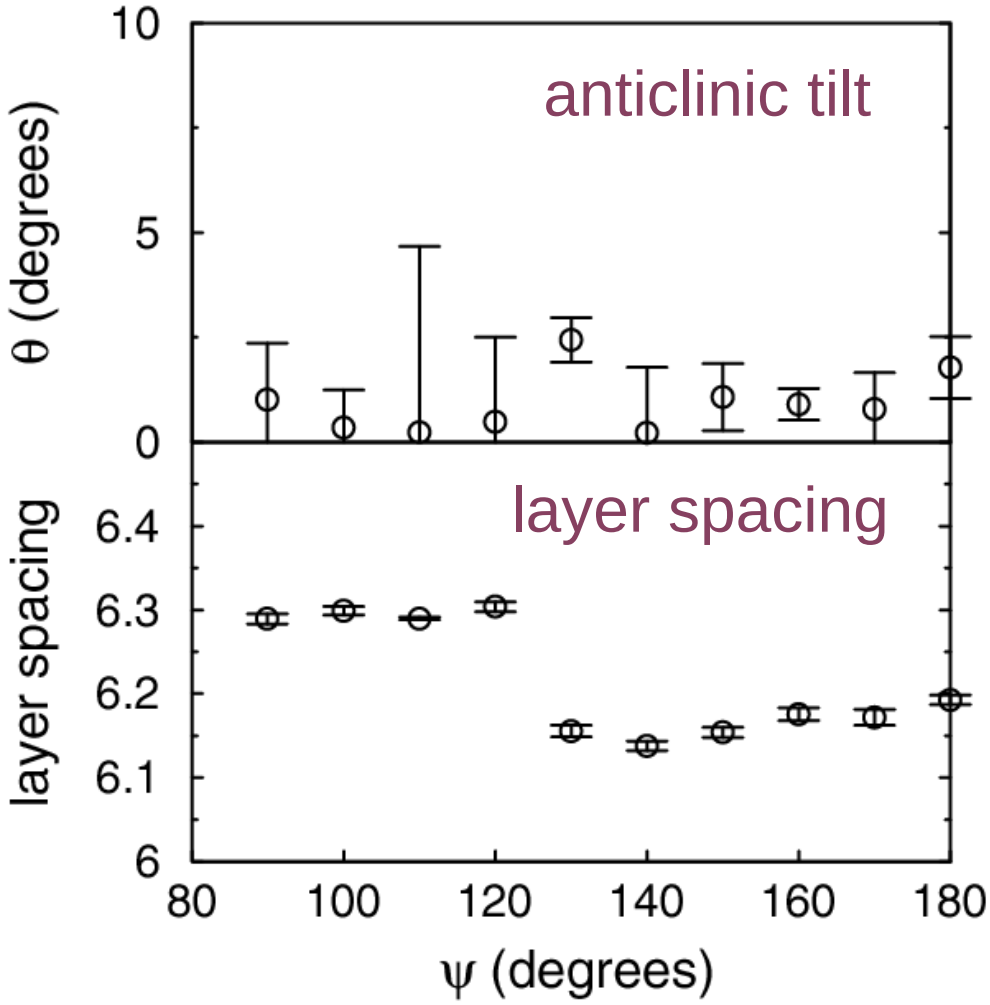

Orientational distributions of bananas for $L_{ban} / D = 2.5$

Molecular director:

$\cos\theta = \mathbf{n} \cdot \mathbf{z}$

Bow vector:

$\cos\theta = \mathbf{m} \cdot \mathbf{z}$

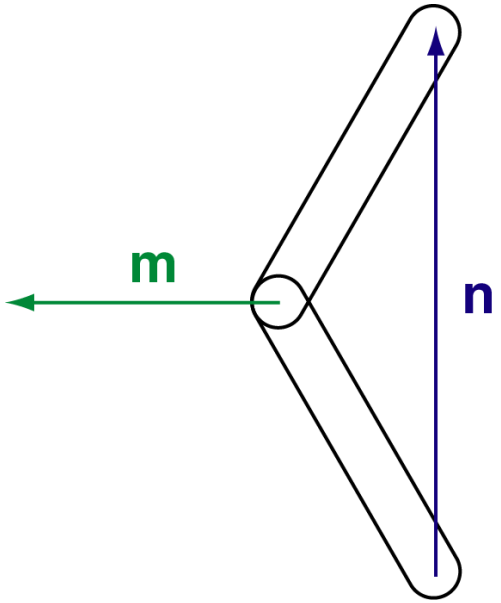

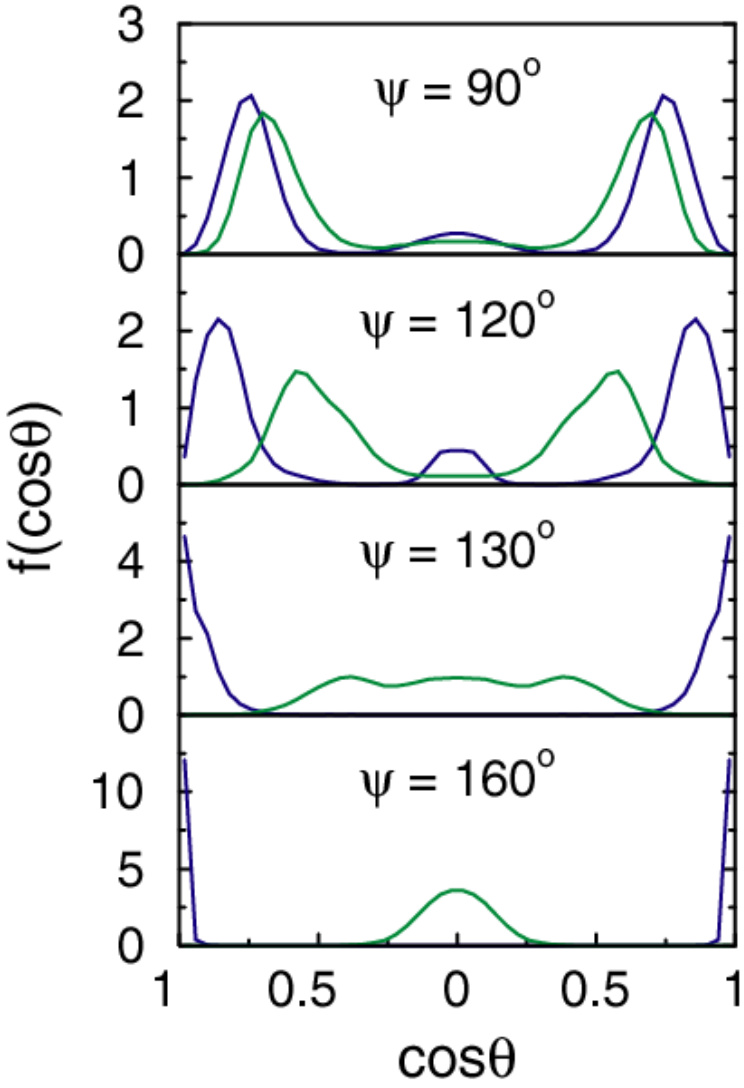

For small opening angles, most banana molecules are ‘half segregated’, with some molecules ‘fully segregated’

Self-assembly in surfactant oligomers

(Molecular Dynamics)

Outline

- Simple model for surfactant oligomers to understand the relationship between molecular structure and the resulting mesophases for surfactant oligomers in solution.
- The thermodynamics of self-assembly of chromonic liquid crystals.
- Surface tension study of the Hexadecane benzene sulfonate
- Coarse grained description for Hexadecane benzene sulfonate

Goal

- To gain a deeper understanding of the various parameters which cause different supramolecular aggregates to form.
- To design molecules with specific aggregate properties.
- Qualitatively study the phase behavior
- To compare our simulation results with available experimental results to validate our model

Ref:

Self-Assembly in surfactant oligomers: A coarse-Grained description through Molecular Dynamics Simulations, *Langmuir*, 18, 1908 (2002)

Isodesmic self-assembly in lyotropic chromonic systems, *Liquid Crystals*, 29, 619 (2002)

Molecular dynamics study of a Surfactant-Mediated Decane-Water Interface: Effect Molecular Architecture of Alkyl Benzene Sulfonate, *J. Phys. Chem. B*, 108, 12130 (2004)

Gemini surfactant: an example of surfactant oligomer

CTMABr

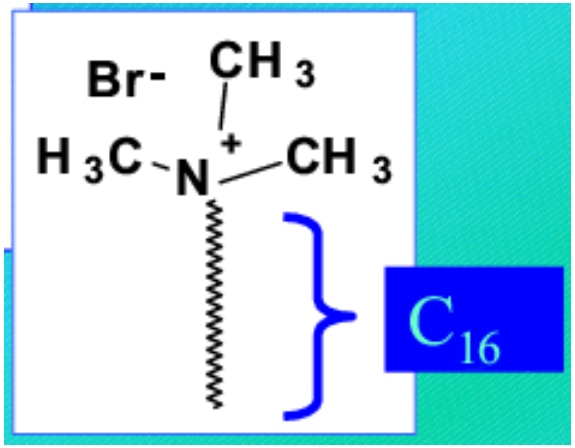

Conventional single tail surfactant

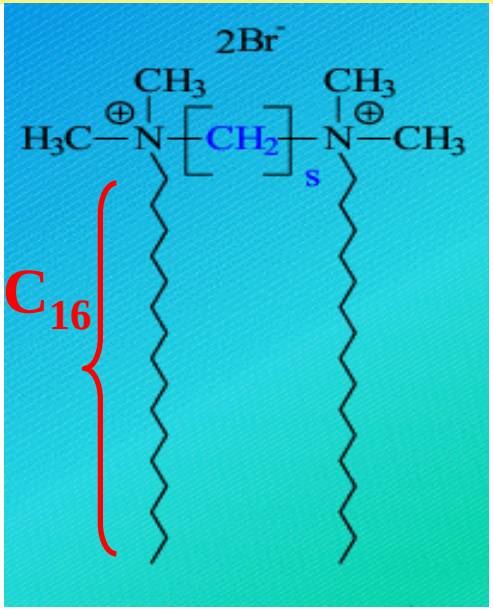

Gemini has two head groups connected by a spacer of variable length

C16-s-16 2Br-)

Some of the advantage of gemini surfactants

- Micellization at low concentration (low CMC)
- Significant decrease in surface tension
- Best efficiency in the adsorption
- Lower value of craft point (better solubility)

Solution of Amphiphiles

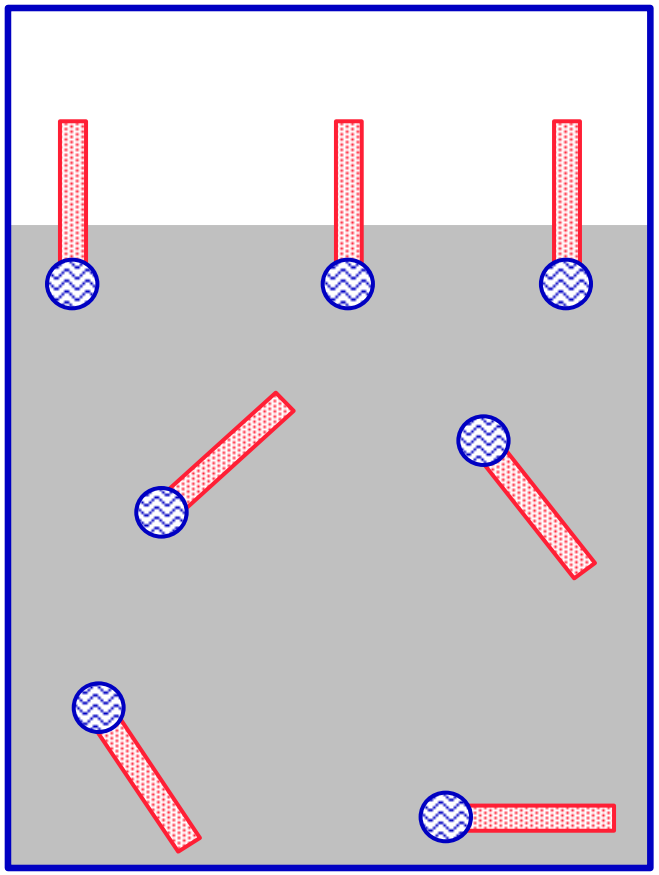

Concentration of surfactant below the critical micelle concentration.

http://www.pharmacy.umaryland.edu/faculty/ghollenb/pchem/colloids/colloids%20revised.ppt

Solution of Amphiphiles

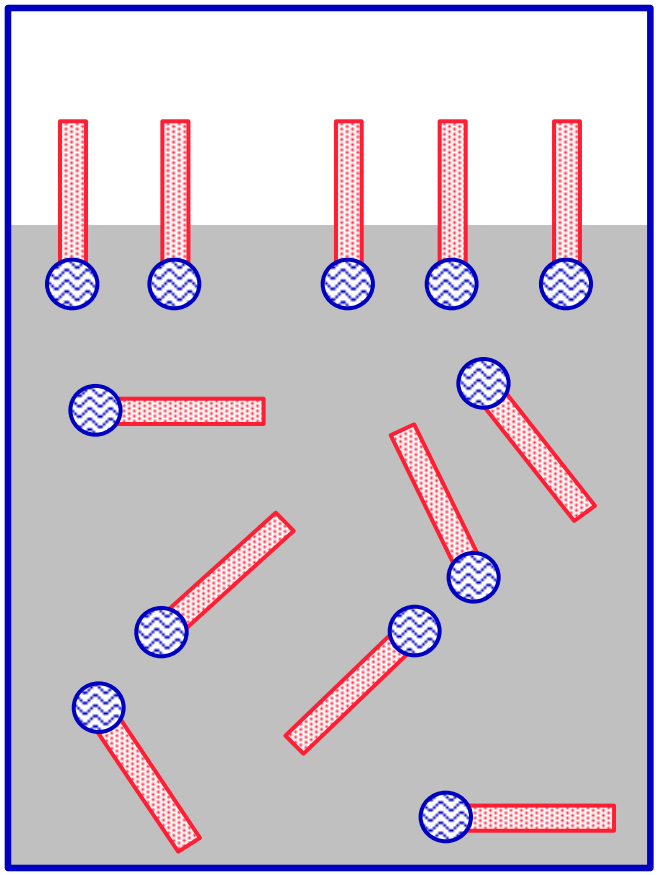

Concentration of surfactant below the critical micelle concentration.

Solution of Amphiphiles

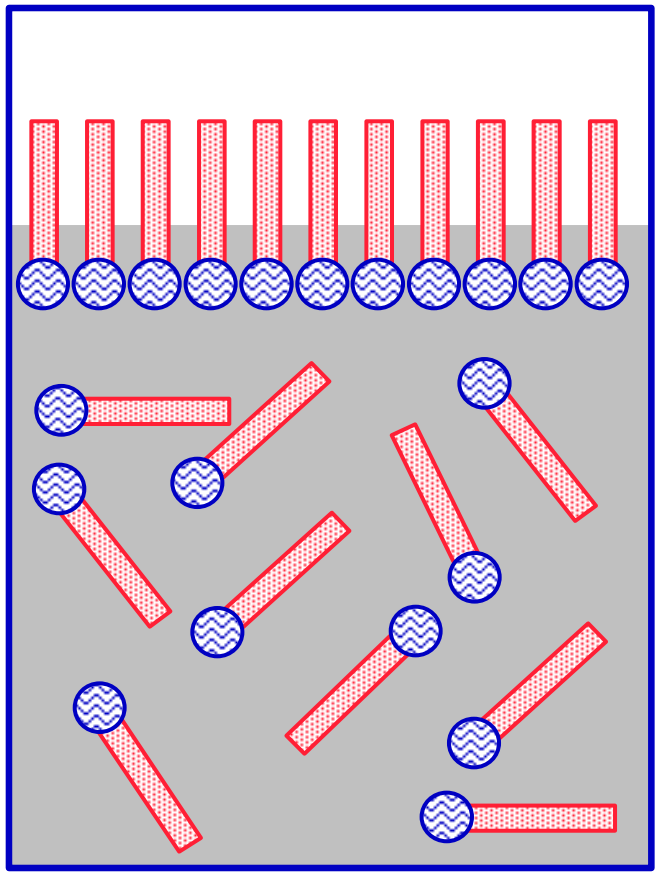

Concentration of surfactant below the critical micelle concentration.

Association Colloids

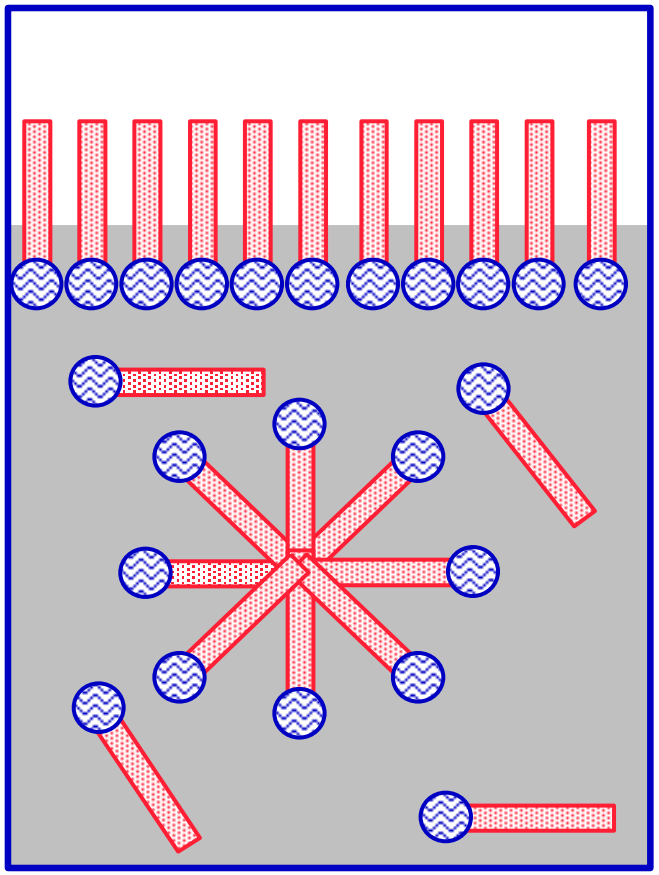

Concentration above the critical micelle concentration.

Phase diagram

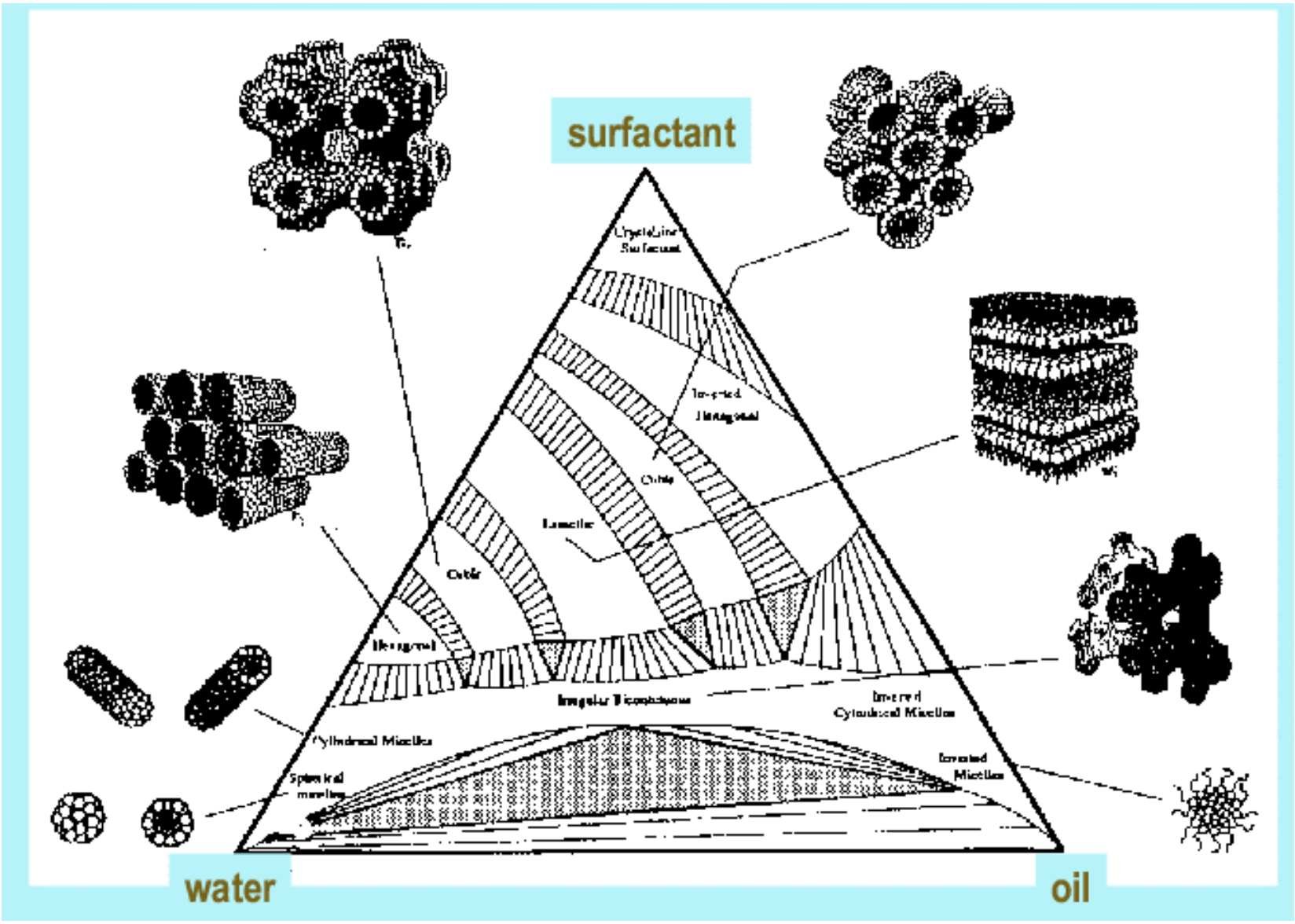

JCP, 91,2479 (1989)

Gemini surfactant: Our previous modeling efforts

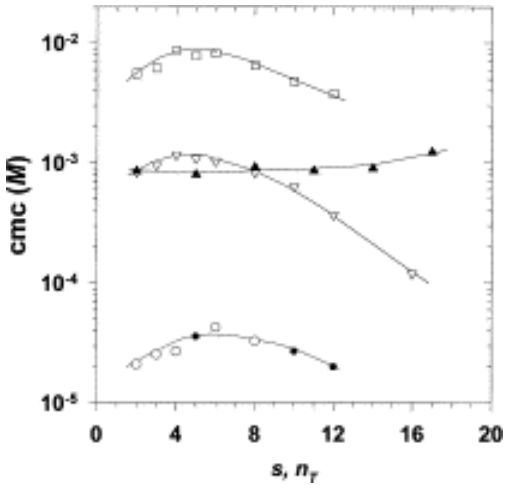

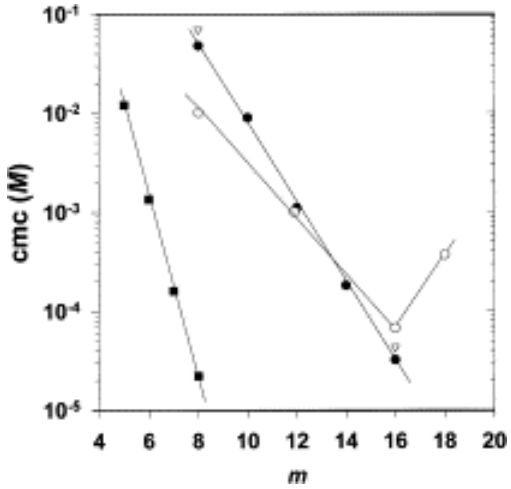

Zana, Adv. Coll. Interface Science, 29, 203 (2002)

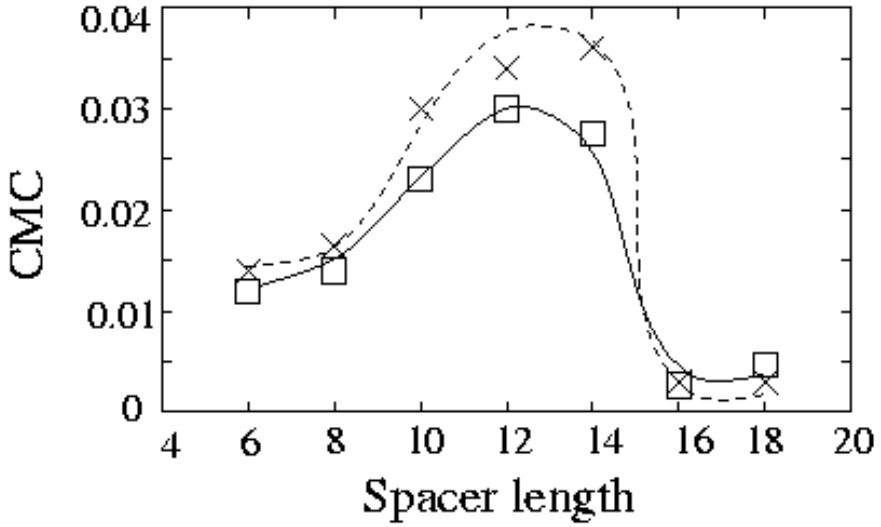

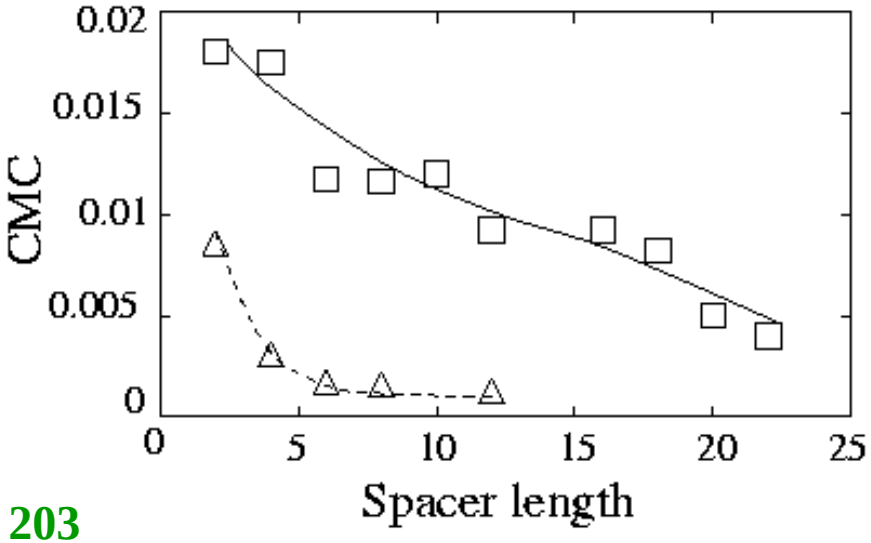

Maiti et. al. EPL, 41, 183 (1998)

Gemini surfactant: Our previous modeling efforts

Cross-linked micelles

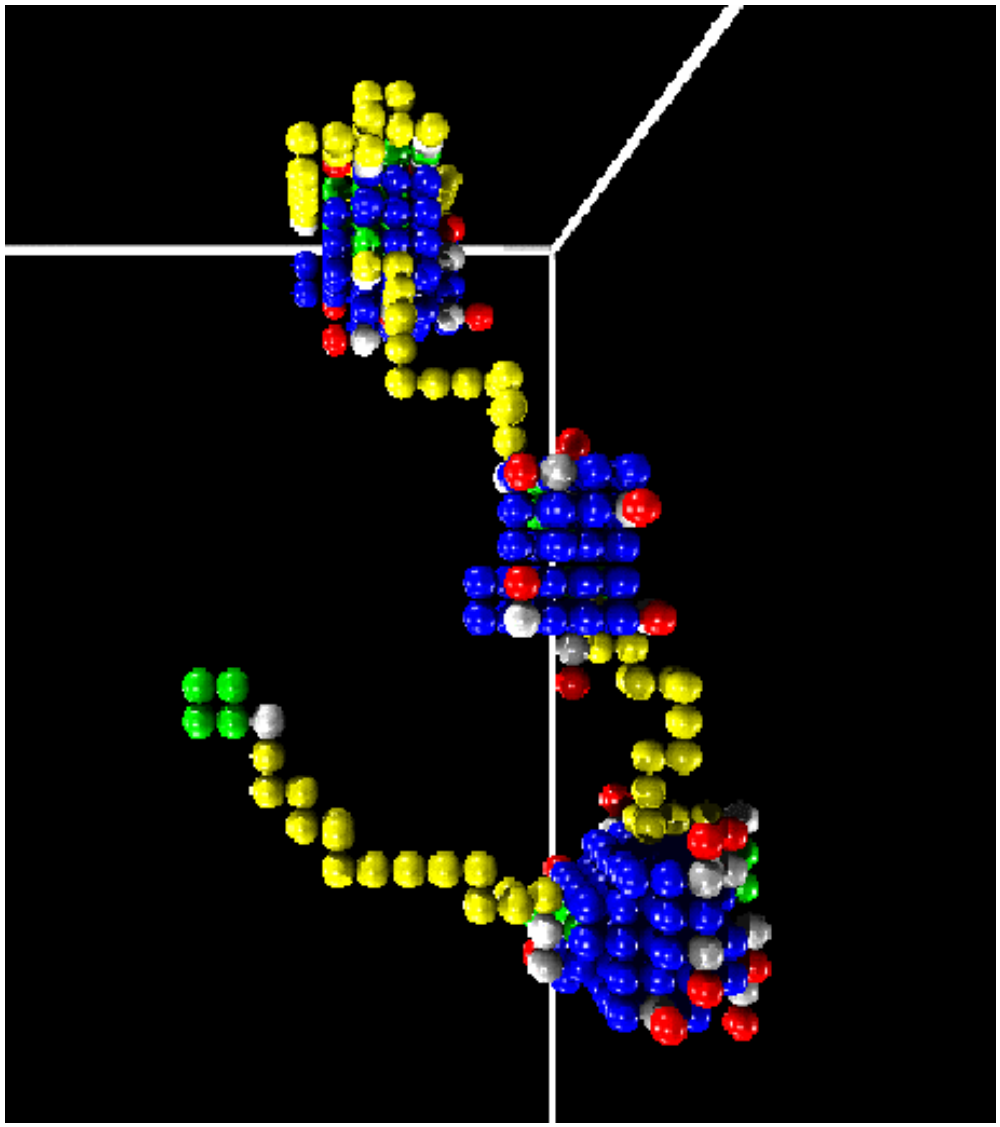

Maiti et. al. Langmuir, 16, 3784 (2000)

Model

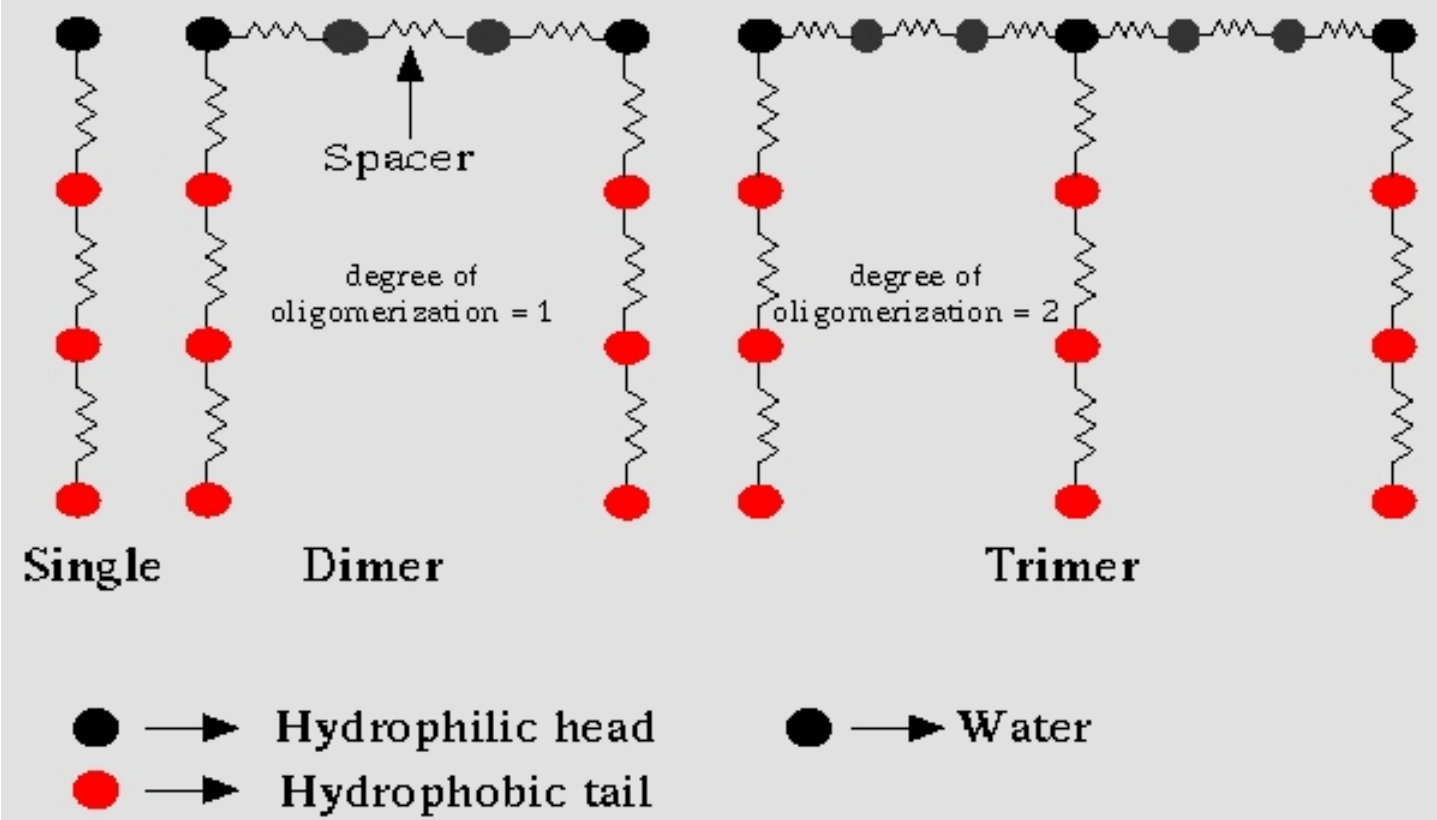

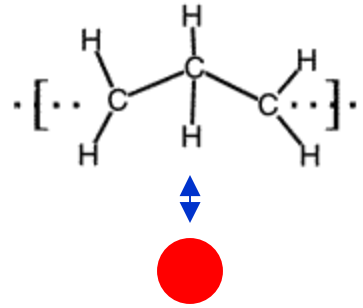

Hydrophobic-water, hydrophilic-hydrophobic interactions: repulsive WCA potential:

$$V_{LJ} = 4\varepsilon\left[\left(\frac{\sigma}{r}\right)^{12} - \left(\frac{\sigma}{r}\right)^{6}\right] + \varepsilon \quad \textit{for } r < r_c = 2^{1/6}\sigma$$

$$= 0 \qquad \textit{for } r > r_c = 2^{1/6}\sigma$$

Water-water, hydrophilic-water, hydrophilic-hydrophilic interactions - attractive Lennard-Jones (LJ) potential:

$$V_{LJ} = 4\varepsilon\left[\left(\frac{\sigma}{r}\right)^{12} - \left(\frac{\sigma}{r}\right)^{6}\right]$$

Model

Neighboring particles of the chain are connected by harmonic spring and interact via a harmonic potential given by

$$V(r) = \frac{1}{2} k \left(r - r_0 \right)^2$$

We have performed MD simulation with constant pressure (NPT) using Berendsen manostat with variable box shape. Temperature was kept constant using Berendsen thermostat (weak coupling to a external heat bath)

Parameters:

- Between N=25,000 and 35,000 particles with Nw water molecules and Ns surfactant molecules of length Ls
- Ls = 5 for single chain surfactant, 12 for dimeric surfactant, 19 for trimeric surfactant
- $T^* = 1.0$, $P^* = 1.0$, $\sigma = 1$, $\varepsilon = 1.0$, $k = 30$, $r_0 = 1.2\,\sigma$
- 2-3x105 MD steps for equlibriation and another 105 steps for production (velocity verlet algorithm with dt between 0.005-0.01)
- Surfactant mole fraction c = Ns/(Ns+Nw)
- Surfactant monomer fraction cs = NsLs/(NsLs+Nw)

Movie time: Micelle formation

Correspondence to real units:

3-4 CH2 groups making one tail bead

So 0.31nm < σ < 0.37nm

0.42kJ/mol < ε <3.5 kJ/mol

We use σ = 0.34 nm

ε= 2.5 kJ/mol

M = 36 g/mol

$\delta t = (m \sigma^2/ \varepsilon)^{1/2}$= 1.3 ps

T = 300K

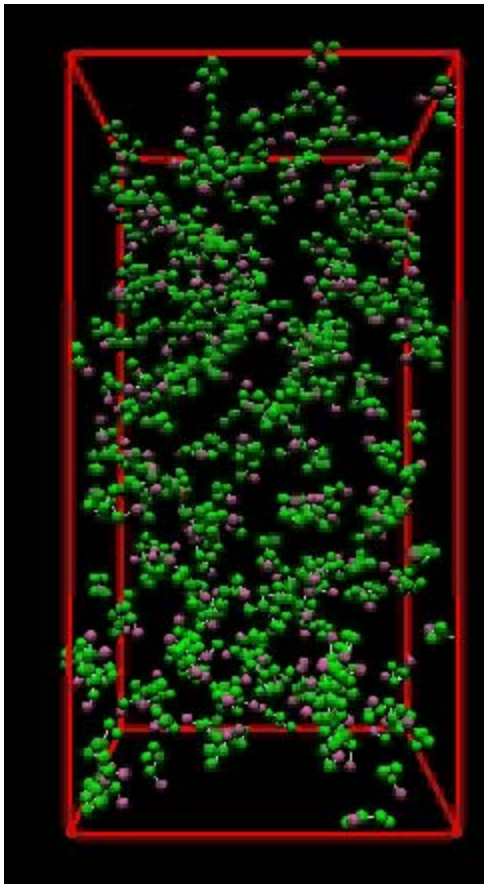

Formation of micelles in a solution containing single chain surfactant
c =0.056

Equilibrium structure at different conc.:

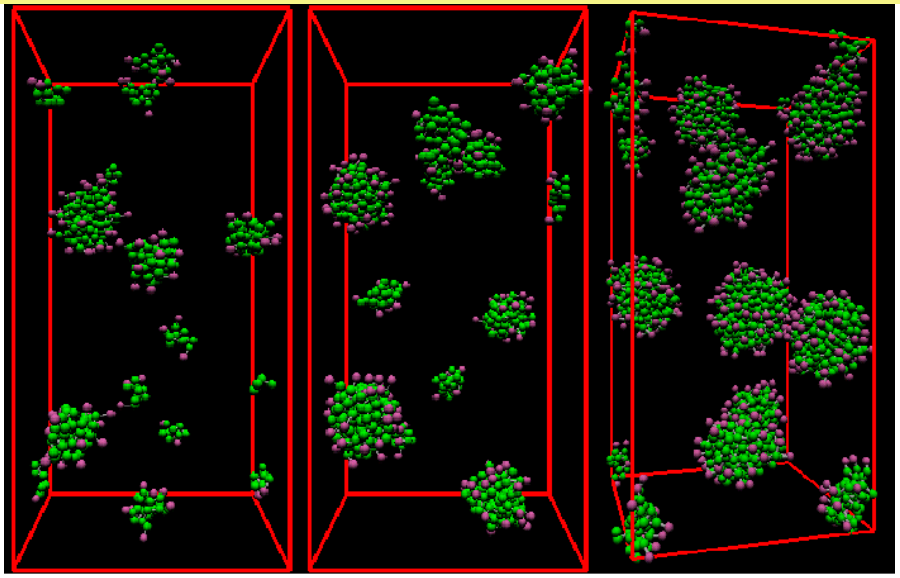

Single chain surfactant

Dimeric surfactant

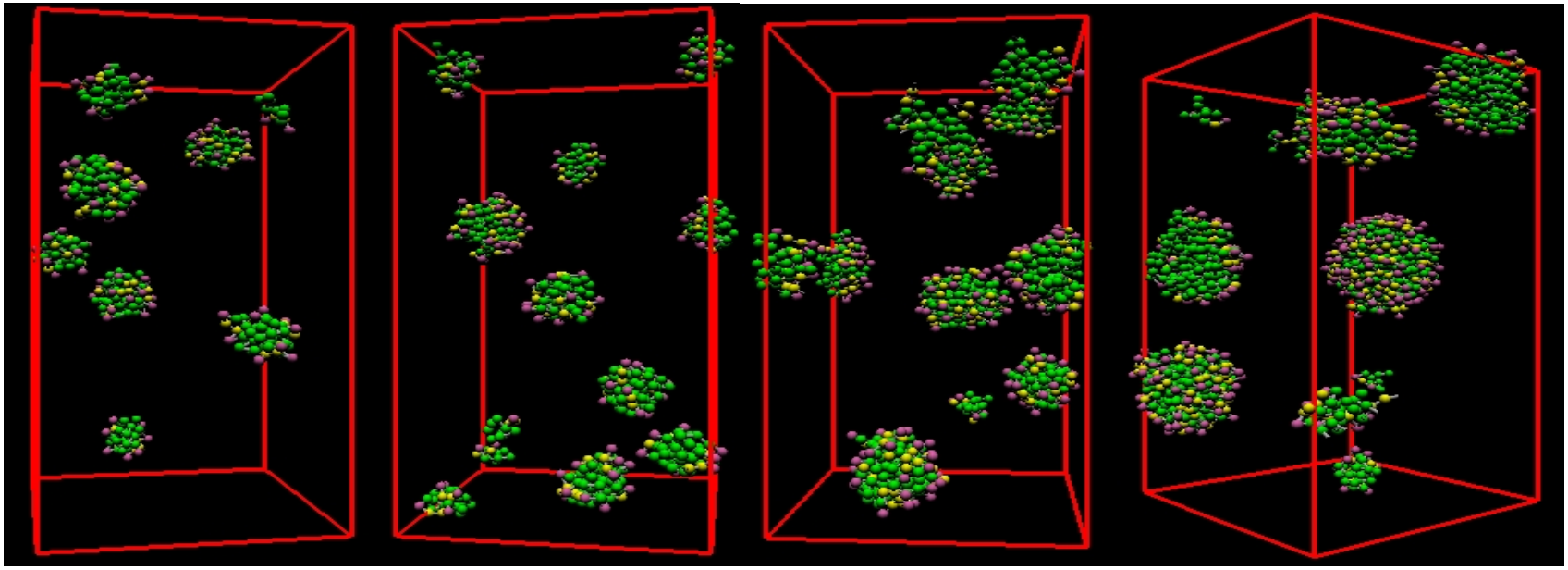

c = 0.000208 **c = 0.002618** **c = 0.00497** **c = 0.00719**

Critical Micellar concentration (CMC)

Various ways to determine CMC in simulation:

- **Plot Free surfactant mole fraction as a function of surfactant mole fraction c and fit it to a line of unit slope. The point at which slope changes corresponds to CMC.**

- **Monitor the change in physical property of micellar solution (like concentration of the solution) as a function of the surfactant mole fraction. Change in the slope corresponds to CMC**

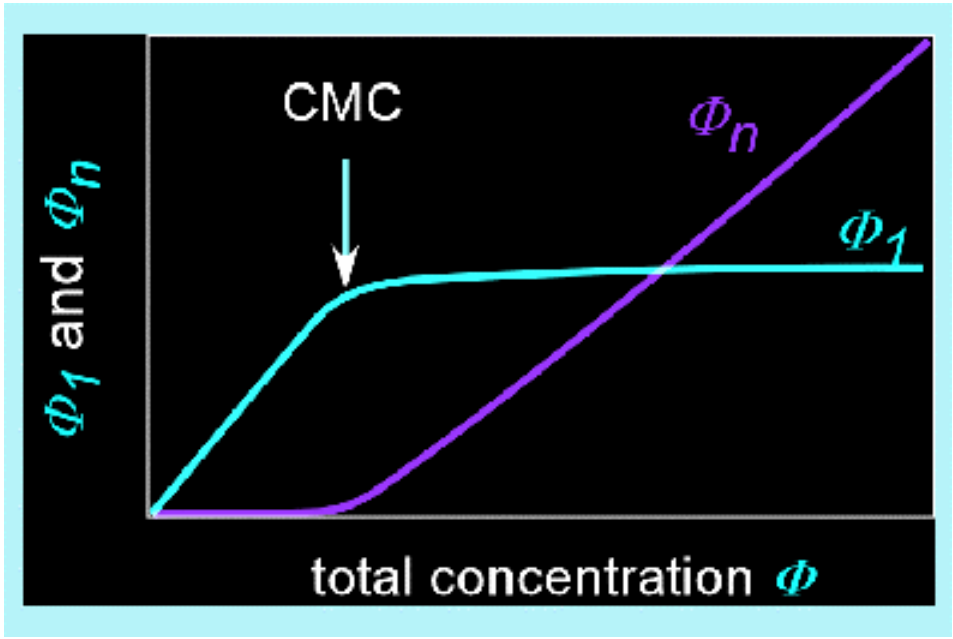

Critical Micellar concentration (CMC)

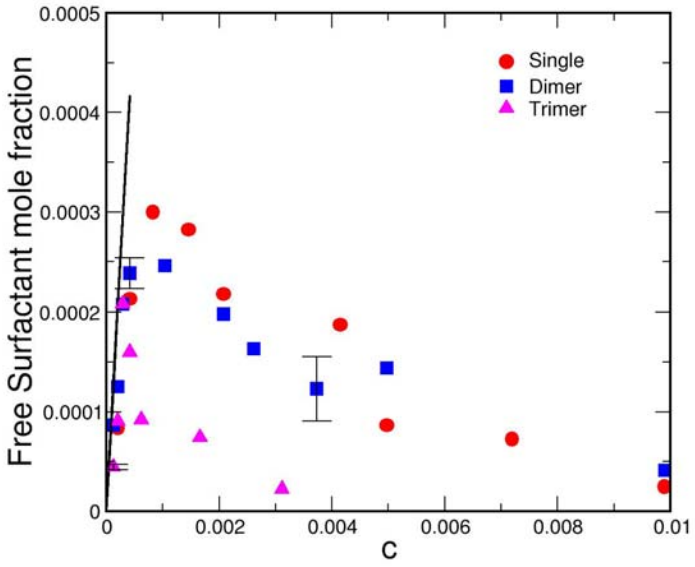

Free surfactant mole fraction as a function of surfactant mole fraction c. The solid line of unit slope is the results for a solution of monomer only

As the solvent molecules are replaced by long surfactant molecules, the volume increases to maintain the same pressure resulting decrease in density. Below CMC individual chain collapse onto itself. Above CMC inside cluster they are much more elongated. This leads to the change in slope of the density plot.

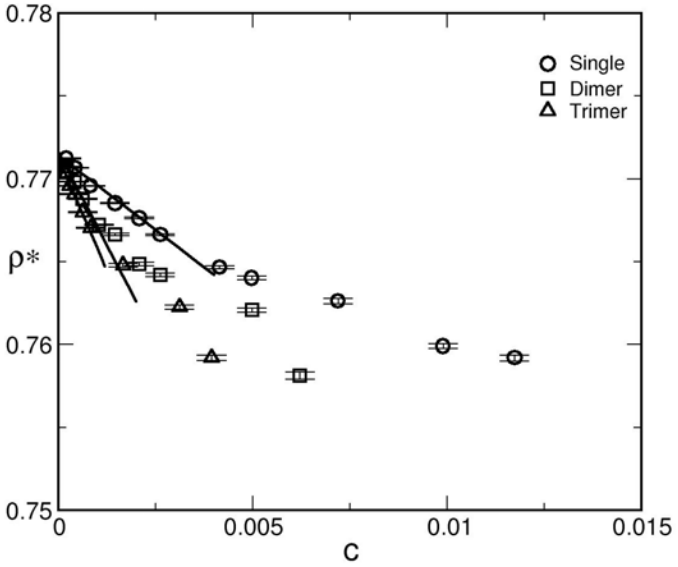

Total number density ρ* as a function of surfactant mole fraction

Critical Micellar concentration (CMC)

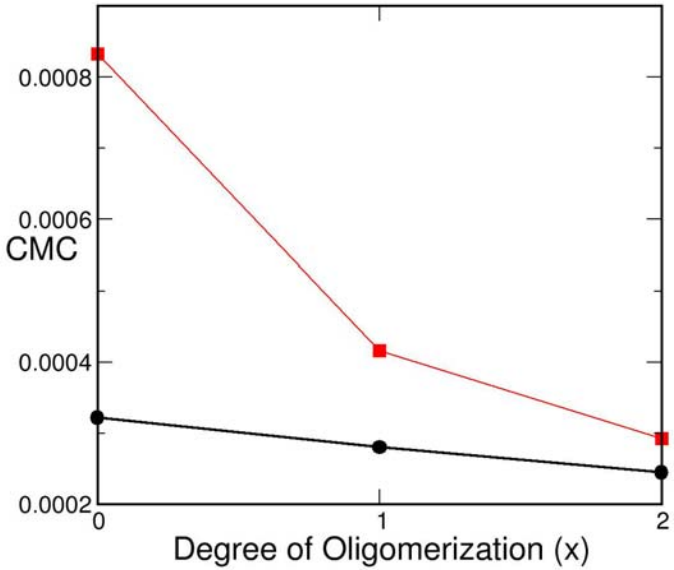

Dimeric (Gemini) surfactant have remarkably low cmc's compared with the corresponding monomeric surfactant of equivalent chain length. For trimeric surfactant it is even lower. These are in qualitative agreement with avialable expt. Data.

Critical Micellar concentration (CMC)

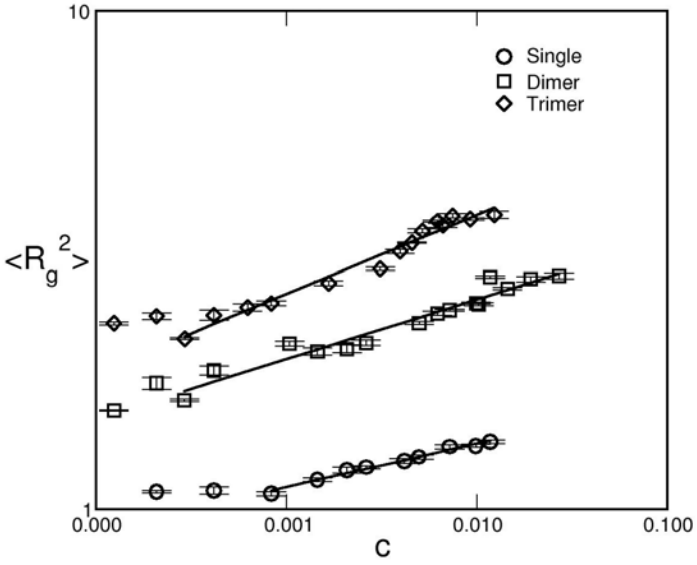

R_g of an individual surfactant increases as a function of surfactant concentration. As an increasing number of surfactants are incorporated in the micelles, they become elongated and the volume occupied by a surfactant is larger for higher aggregation numbers. So the volume excluded to a free monomer due to the presence of free surfactants is more than the volume excluded to a monomer by an aggregate formed by the surfactants. So larger aggregates are favored since they reduce the total excluded volume.

Micelle size and Shape

The shape tensor of the micelle

$$G_{mn} = \frac{1}{S}\left[\sum_{i}^{S}\left(r_{mi} - R_m\right)\left(r_{ni} - R_n\right)\right], m,n = x,y,z$$

S cluster size and R CM of the cluster

Ratio of the eigenvalues of G (g_1, g_2, g_3 in descending order) determine the shape of the micelles. And sum of them give $<R_G^2>$.

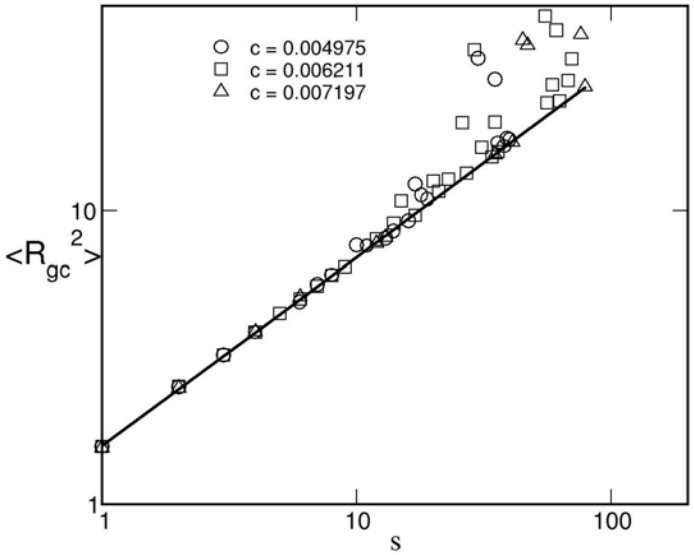

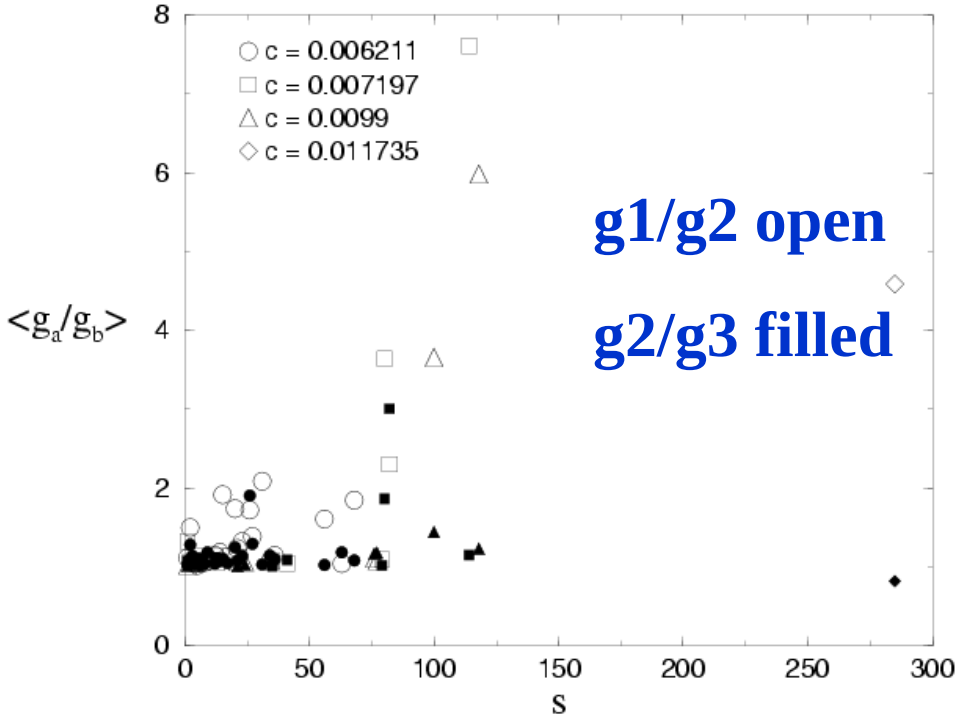

g1/g2 open

g2/g3 filled

R_{gc} ~ $s^{1/3}$. This indicates almost Spherical shape in this conc. regime

For Ns<75, g1/g2 ~1.1-2.0

And g2/g3 ~ 1.1-1.3

Micelle size and Shape

Average cluster size $\langle L \rangle_W = \frac{\sum_s s^2 N(s)}{\sum_s s N(s)}$

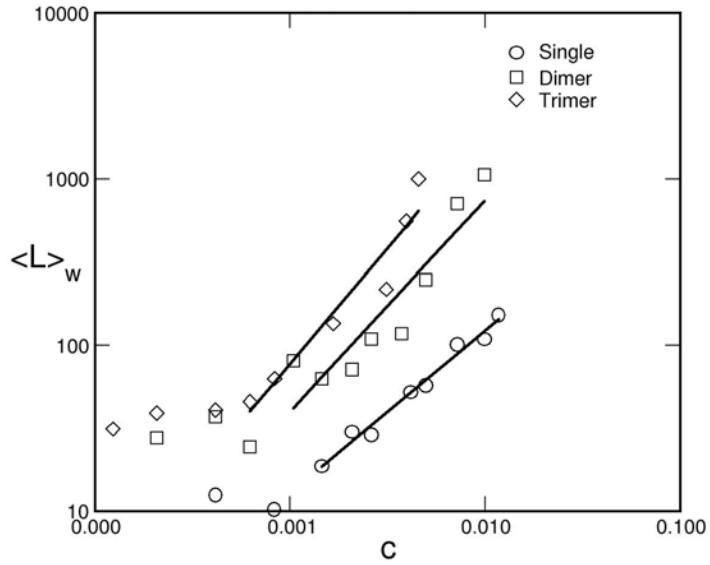

$\langle L \rangle_W \sim c^{\alpha}$ **for c >>cmc**

α= 0.98 +/- 0.06 for single chain

α= 1.27 +/- 0.22 for dimeric

α = 1.39 +/- 0.19 for trimeric

Our growth exponent is very close to the prediction by Schurtenberger et. al. Langmuir, 12, 2894 (1996)

For dimeric and trimeric surfactants, the repulsive interactions between the head groups are screened due to the presence of spacer groups and the micelle size can grow faster compared to their single chain counterpart.

Sphere to cylinder Transition

As the concentration is increased due to the screening of repulsive head group interactions the surfactant now have a preference for local cylindrical packing.

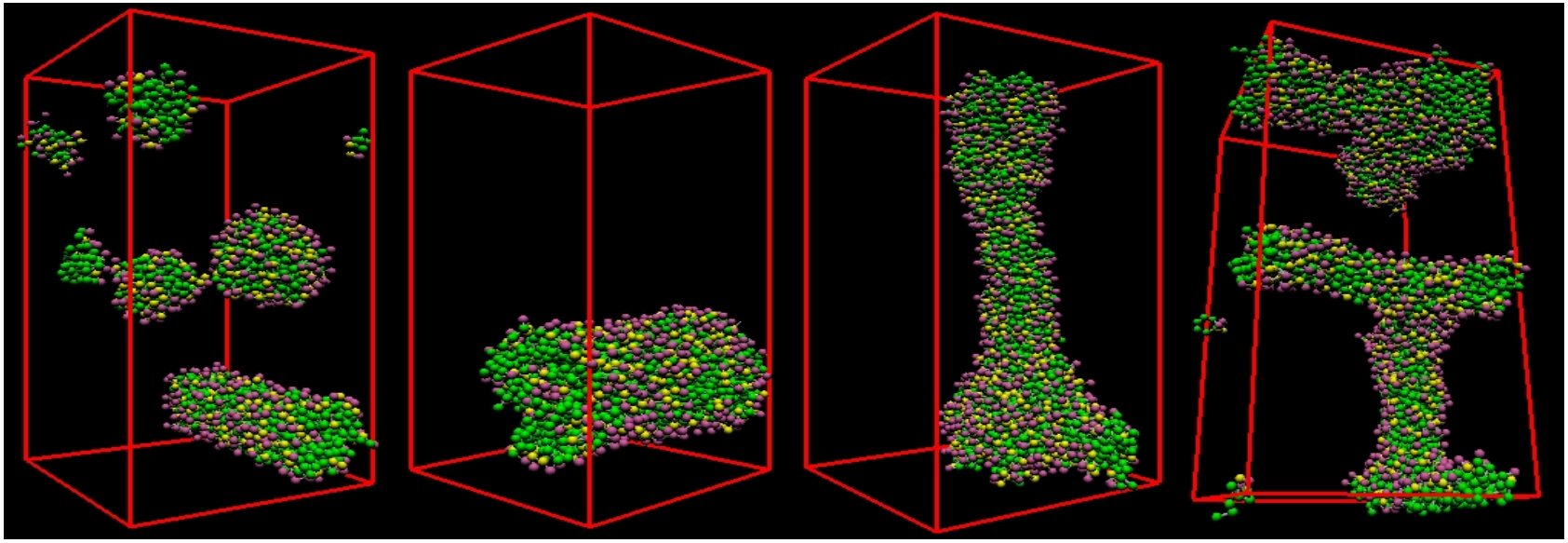

c = 0.0099 **c = 0.011735** **c = 0.0144** **c = 0.0192**

Closed-Loop micelles

Formation of closed loop micelles in worm-like micellar system has been theoretically predicted and observed expt. In surfactant tetramer solution Zana et. al. Langmuir, 16, 141 (2000)

Formation of closed-loop micelles require delicate balance between the volume of hydrophobic tail (v), length of hydrophobic tail (l) and the effective surface area per head group (a) to achieve desired packing parameter P = v/la. Such fine tuning happens with surfactant oligomers

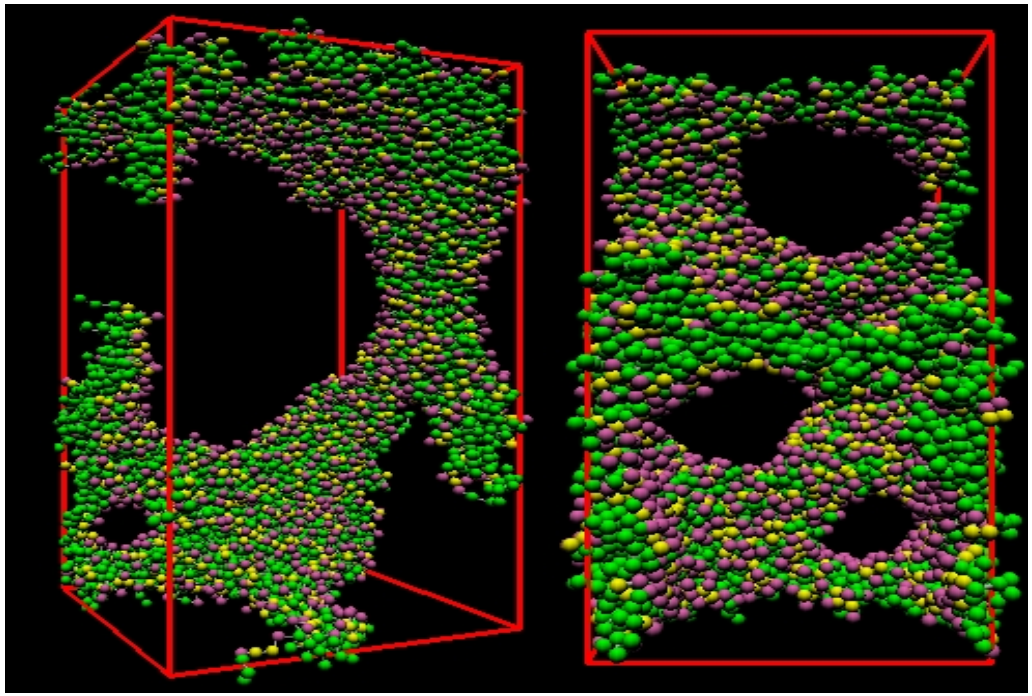

c = 0.027 **c = 0.0345**

Our simulation gives first direct evidence of the formation of closed-loop micelles for both dimeric and trimeric surfactant at intermediate concentration

Structure of micelles

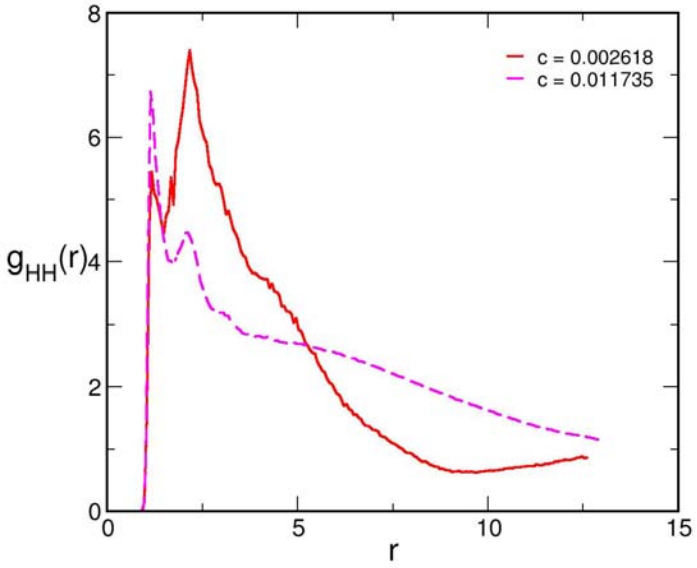

Radial pair correlation function for the head groups for dimeric surfactant at two different conc.

C = 0.0026 (spherical micelles)

C = 0.011735 (cylindrical micelles)

- **Closer packing of head groups in cylindrical micelles (larger 1st peak)**
- **In spherical micelles head groups are surrounded by water (appearance of second peak) apart from other heads.**

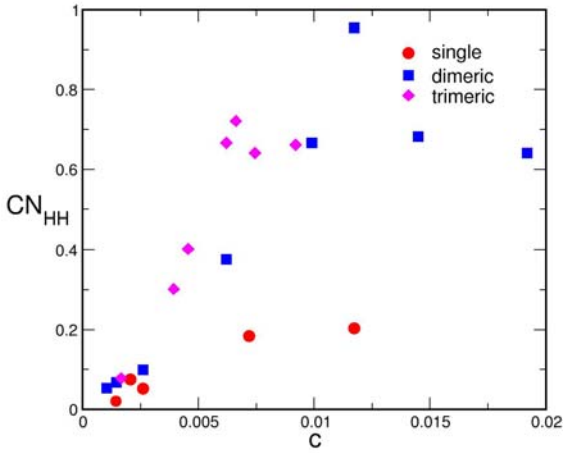

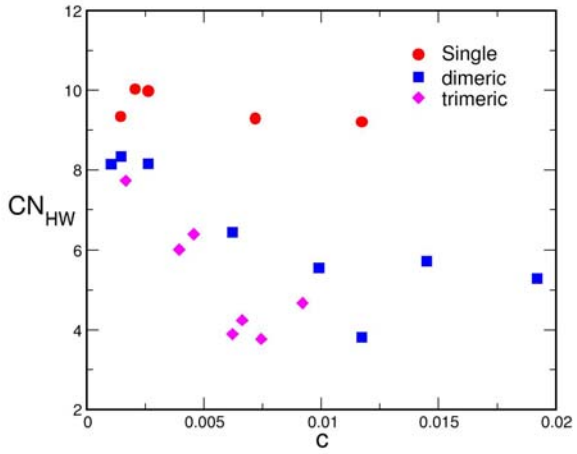

Diffusivity

Diffusion constant D is related to the mean-square displasement (MSD) by

$$D=\frac{\sum\left[r_i(t)-r_i(0)\right]^2}{6N_a t}$$

$R_i(t)$ and $r_i(0)$ are the CM of i-th chain at time t and t=0 respectively

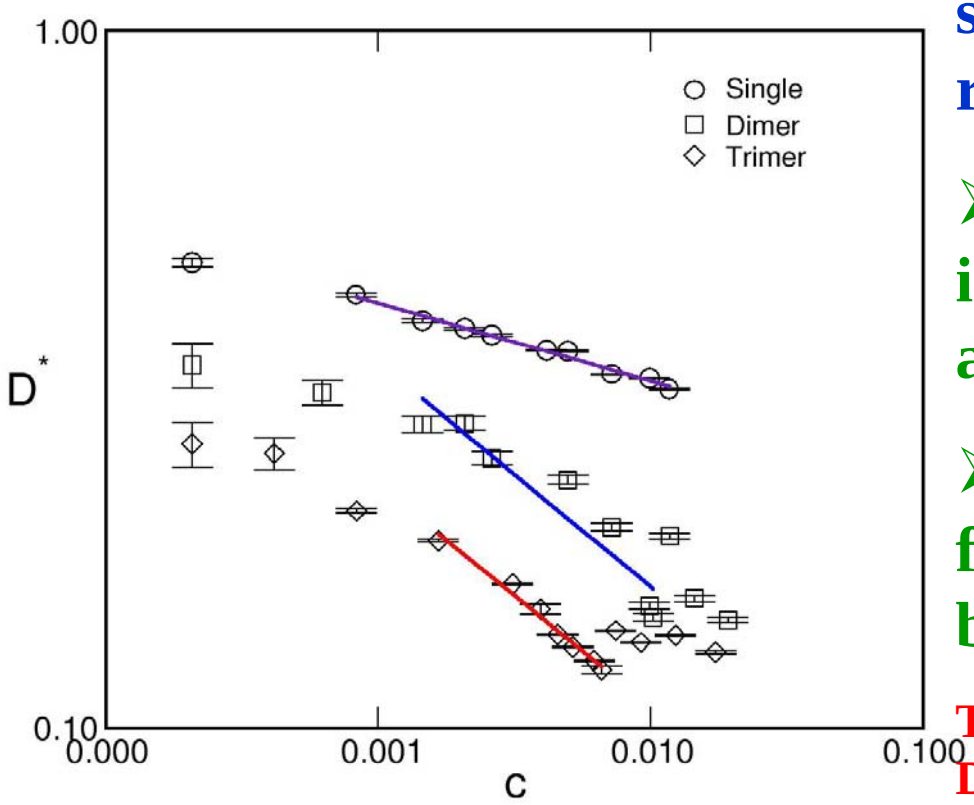

For dimeric and trimeric surfactant D* shows two distinct regimes:

- **For low c D* remains independent of c. Here micelles are spherical shape.**
- **After that D* decreases very fast following $c^{-\delta}$ with δ =0.38 for both dimeric and trimeric**

This is in qualitative agreement with expt. Data Zana et. al. PRL, 81, 228 (1998)

Self-assembly in Lyotrpic Chromonic systems

(Rigid body Monte Carlo)

Motivation

The thermodynamics of self-assembly of chromonic liquid crystals is poorly understood

- **Chrmonic LCs differ significantly from conventional aliphatic lyotropics.**
- **Hierarchical self-assembly**
- **Self-assembly of columnar aggregates is thought to be isodesmic (in contrast to conventional aliphatic lyotropics)**

Dichoric thin films formed from chromonic LCs can be used both as alignment layers and polarizers for LC cells

Oleg Lavrentovich, LCI, Kent State University

Novel materials composed of plank- or disk-like molecules in organic solvents (lyomesophases, or organic lyotropics) exhibit similar hierarchical structures.

Various phases formed by chromonic

In contrast to the conventional amphiphilic molecules chromonic molecules are:

- **Plank-like rather than rod-like**
- **Rigid rather than flexible**
- **Aromatic rather than aliphatic**

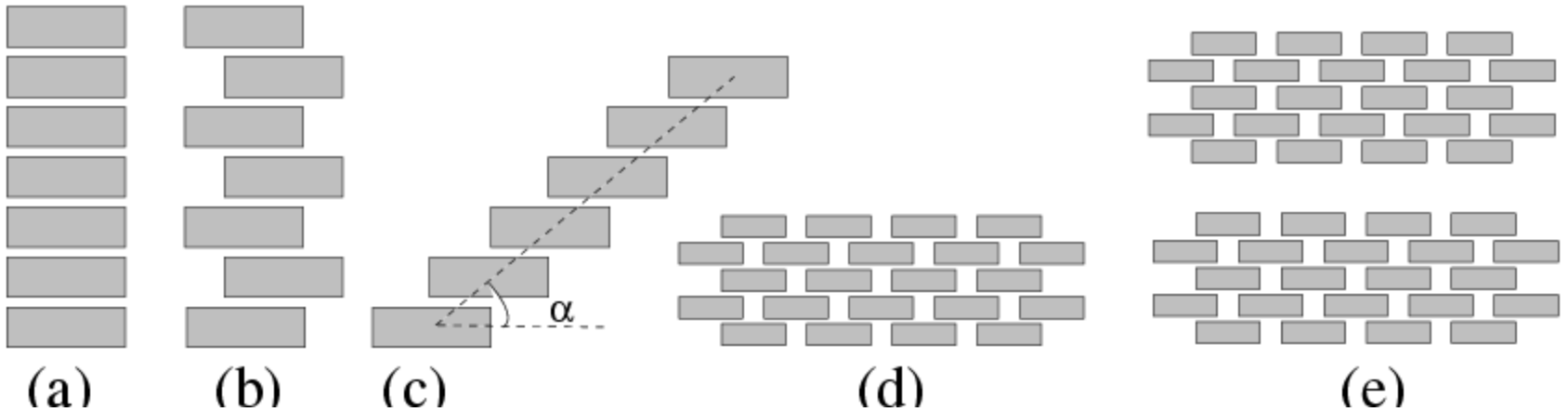

Schematic representations of the chromonic columnar aggregates, H-aggregates (a and b), J-aggregates (c), brickwork structure (d), and layered brickwork structure (smectic) (e).

Contd.

They form isotropic (I), nematic (N) and columnar and hexagonal (M) phases

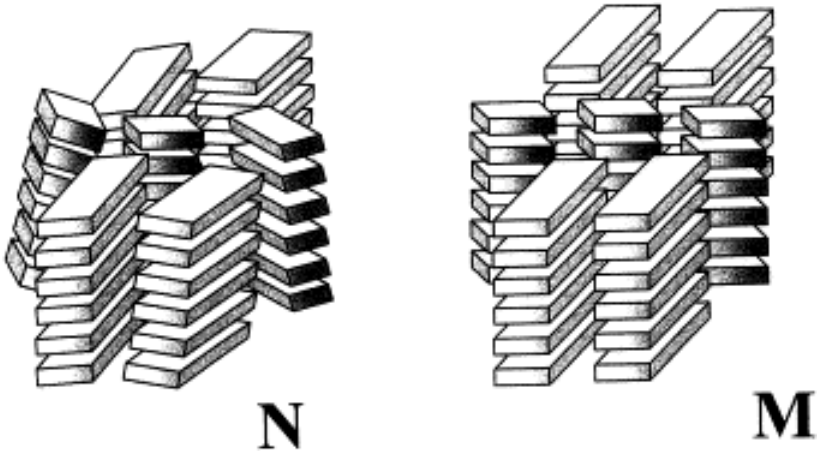

Some of the molecules forming chrmonic phases

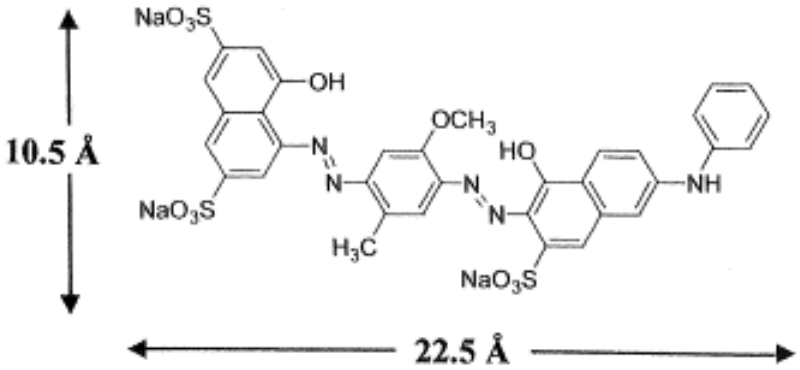

CI Direct Blue. This forms a chrominc N phase

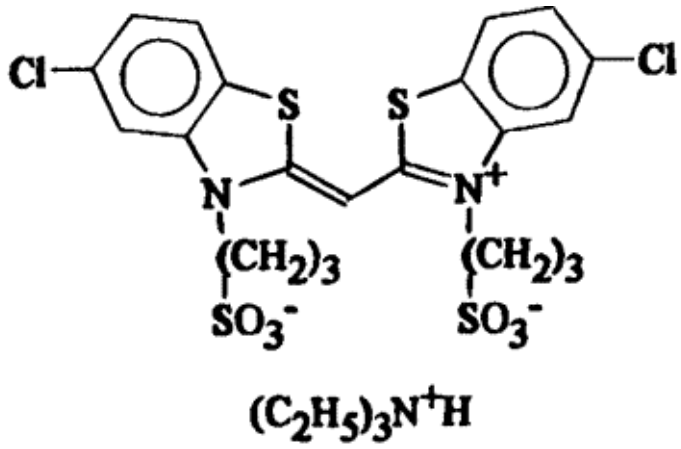

Model building

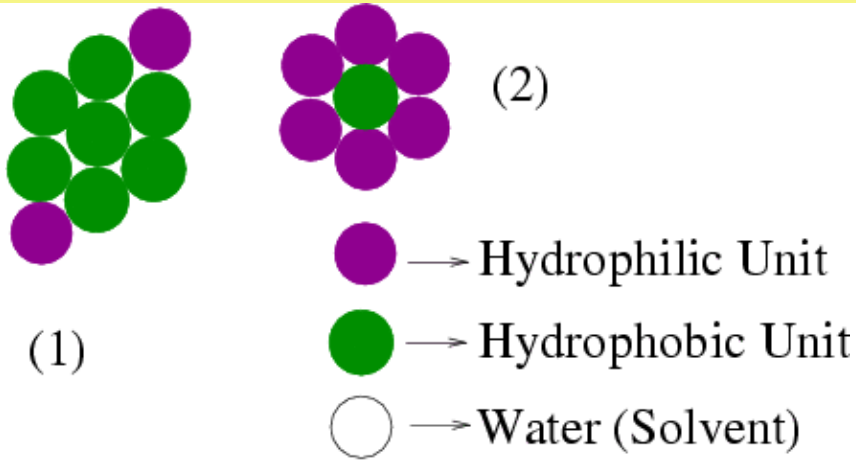

Chromonic –rigid molecules composed of hydrophobic and hydrophilic interaction sites

Solvent –Lennard-Jones fluid

Hydrophobic-water, hydrophilic-hydrophobic interactions: repulsive WCA potential:

$$V_{LJ} = 4\varepsilon\left[\left(\frac{\sigma}{r}\right)^{12} - \left(\frac{\sigma}{r}\right)^{6}\right] + \varepsilon \quad \textit{for } r < r_c = 2^{1/6}\sigma$$

$$= 0 \qquad \textit{for } r > r_c = 2^{1/6}\sigma$$

Water-water, hydrophilic-water, hydrophilic-hydrophilic interactions - attractive Lennard-Jones (LJ) potential:

$$V_{LJ} = 4\varepsilon\left[\left(\frac{\sigma}{r}\right)^{12} - \left(\frac{\sigma}{r}\right)^{6}\right]$$

Simulation details

NPT Monte Carlo (MC) simulations of chromonic/solvent mixtures with varying concentration of chromonic molecules

Each MC moves consists of translation and rotation of chromonic solvent molecules. Rotation is performed through Quaternion.

Simulations carried out at T* =1.0, P* = 1.0, in dense liquid phase of the LJ system

Free energy of association of small chromonic aggregates measured via umbrella sampling to test isodesmic assumption

columnar aggregate formation:

Beginning of chromonic columnar aggregate formation: $\phi = 0.081$, $N_c=50$, $N_w=5100$

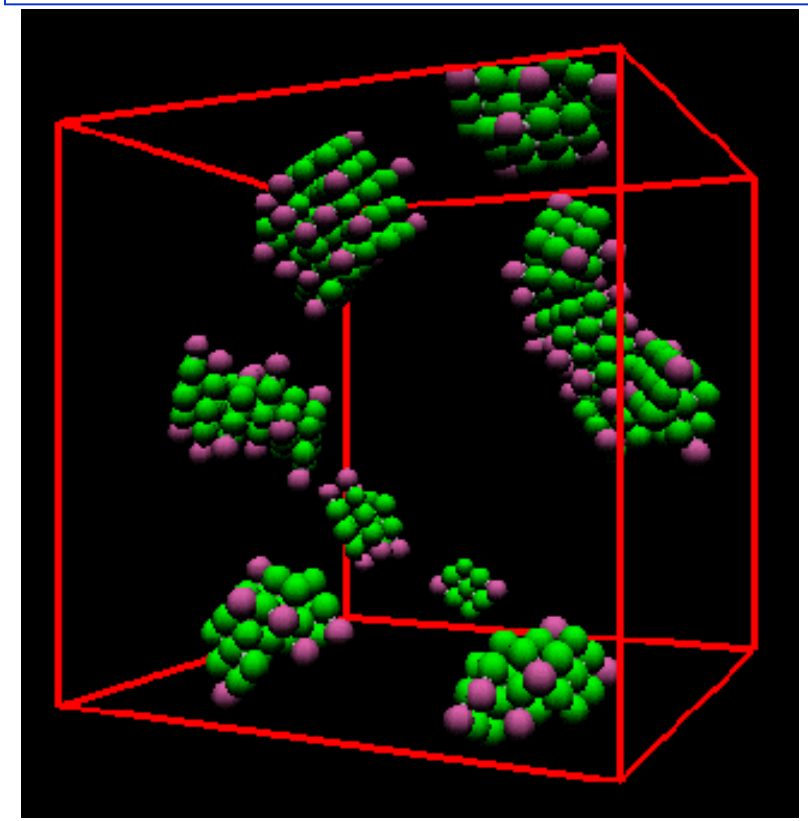

Chromonic columnar aggregate at higher concentration formation: $\phi = 0.081$ ($N_c=90$)

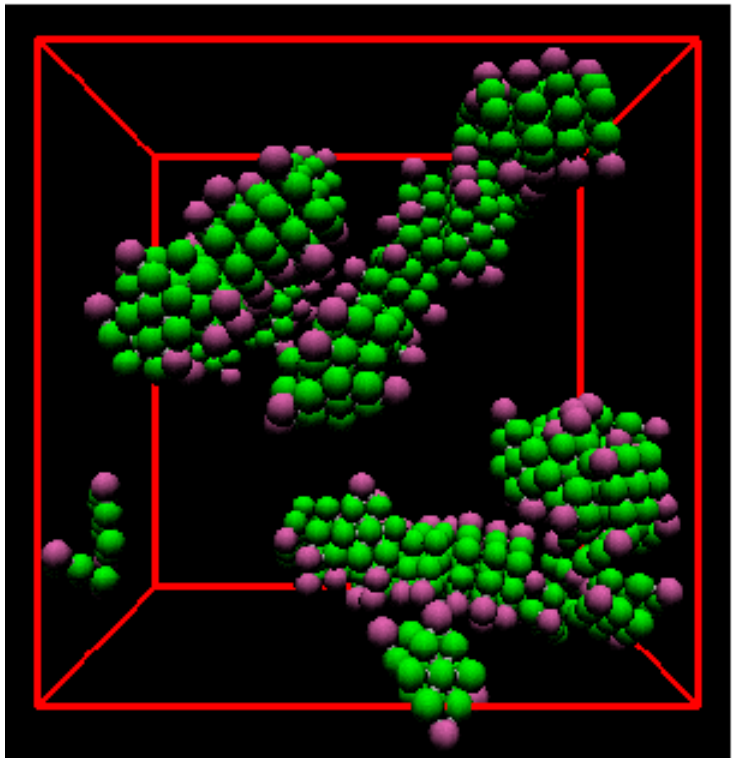

At low conc. The chromonic molecules form short columns, and with increase in conc. The length and number of aggregates increases.

columnar aggregate formation:

To probe the formation of columnar aggregates we compute positional pair correlation function g^{cc} between the CM of chromonic

$$g^{cc}(r)=\frac{1}{\rho N_c}\left\langle \sum_{i\neq j}\delta\left(r-r_{ij}^{cc}\right)\right\rangle$$

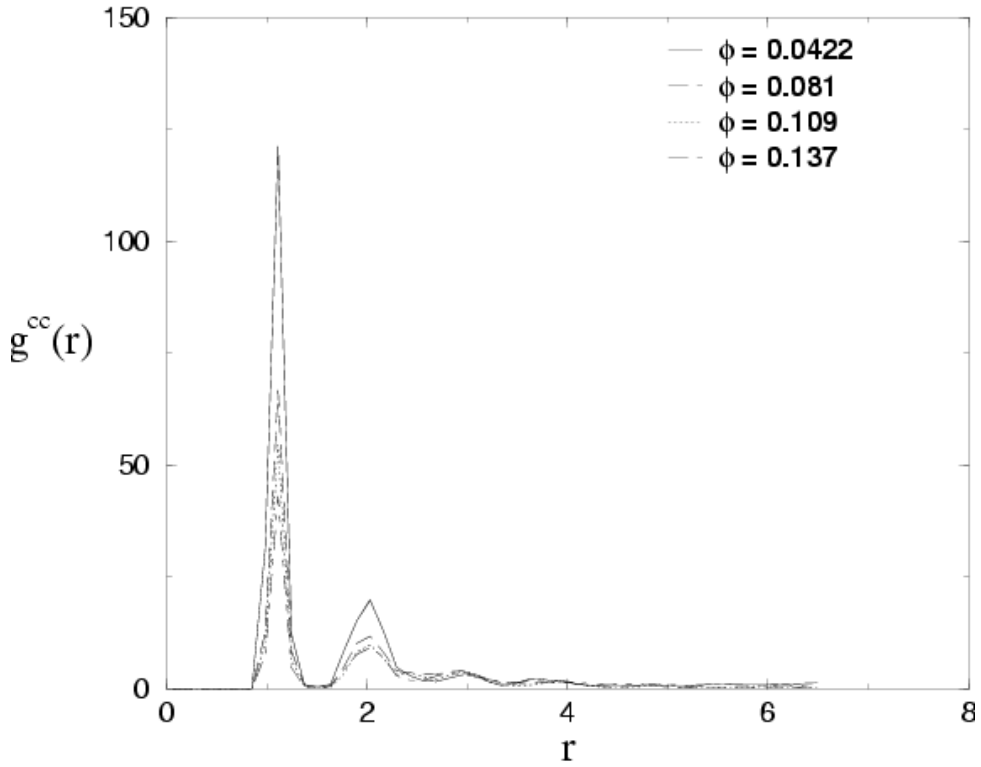

First peak at r = 1.12σ signifies strong positional correlation between chromonic molecules Successive small peaks at r = 2.2 σ 3.3 σ etc indicate they form columnar aggregates.

columnar aggregate formation:

To probe the orientation of chromonic in columnar aggregates we compute Orientatinal correlation function g^{cc} and g_1^{cc}

$$g^{cc}(r_{\parallel},r_{\perp})=\frac{1}{2\pi}\int_0^{2\pi}d\varphi\, g^{cc}(r_{\parallel},r_{\perp},\phi)$$

$$g_1^{cc}(r)=\frac{1}{\rho N_c g^{cc}(r)}\left\langle \sum_{i\neq j} P_2\left(u_i^{cc}\cdot u_j^{cc}\right)\delta\left(r-r_{ij}^{cc}\right)\right\rangle$$

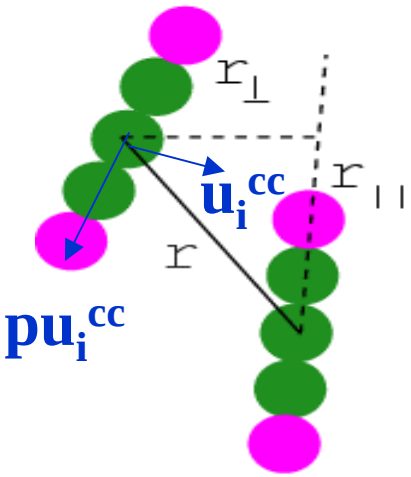

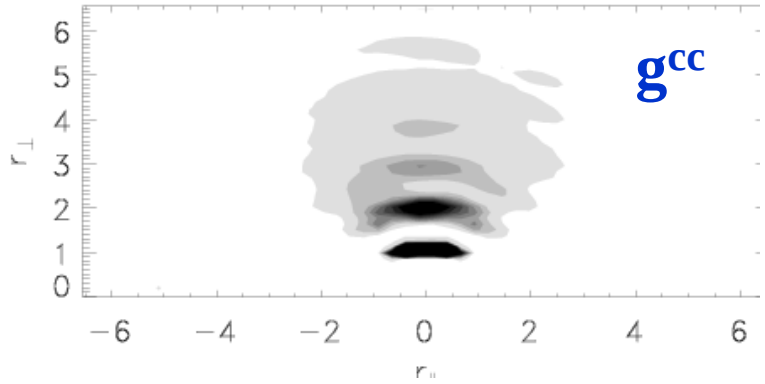

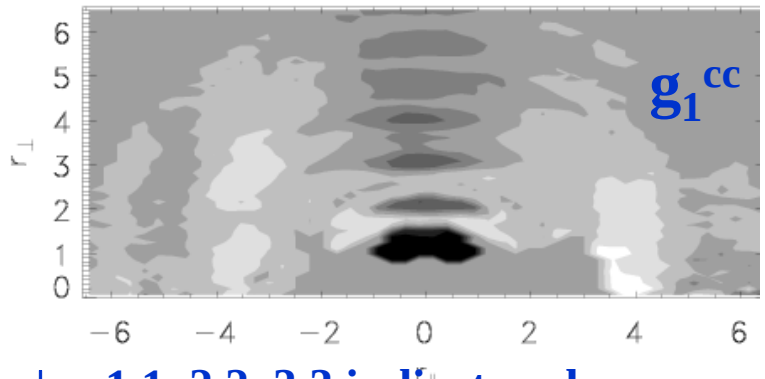

Peaks at r⊥ ~ 1.1, 2.2, 3.3 indicate columnar aggregate. Strong intensity peak around r|| ~ 1.0 indicate parallel arrangement in the column.

Average aggregation number:

Average cluster size $\langle L \rangle = \frac{\sum_s s^2 N(s)}{\sum_s s N(s)}$

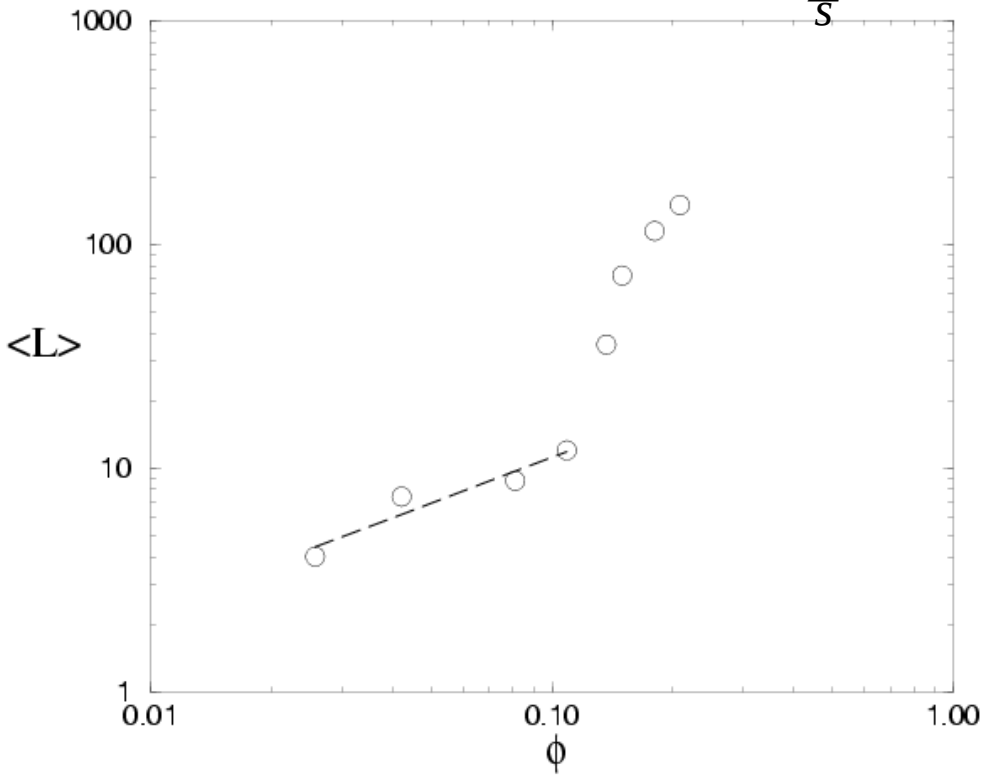

- At low concentration <L> ~$\phi^{0.6}$
- Higher concentration shows stronger dependence on ϕ
- At high conc. Short columns aggregates to form chain like aggregates.
- Chain like aggregates tends to exhibit stronger excluded volume interactions leading to enhance growth of micelles **(PRB, 46, 6061 (1992)**

columnar aggregate formation:

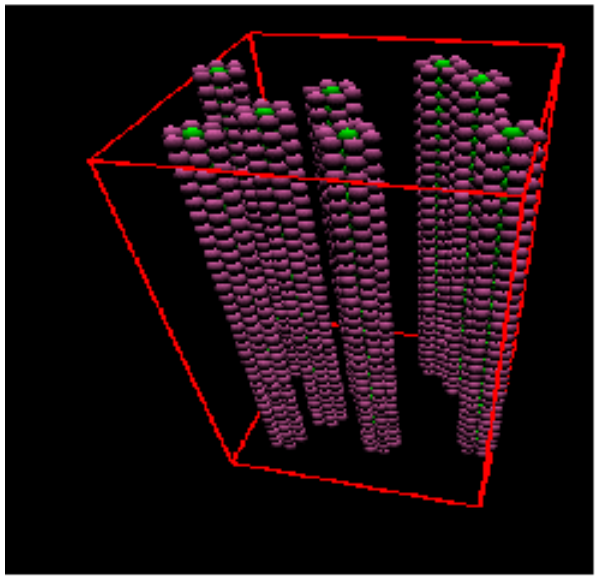

Initial str.

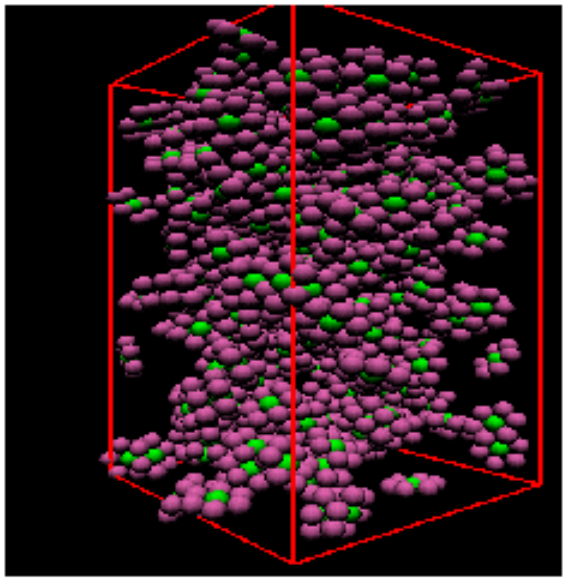

Final str.

Simulation with eight columnar aggregates: at the end of simulation columnar aggregates go to isotropic N_c=256, N_w=2304

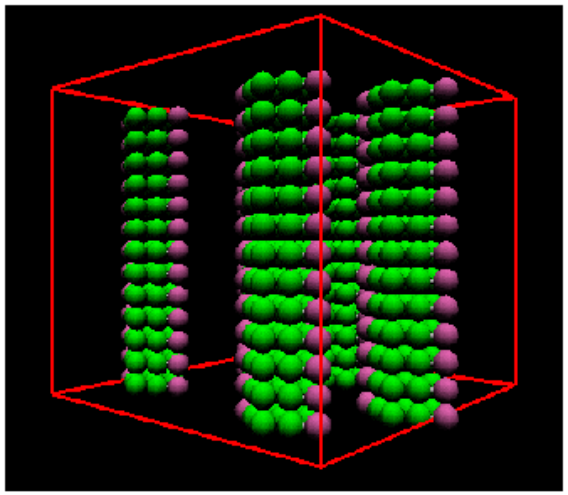

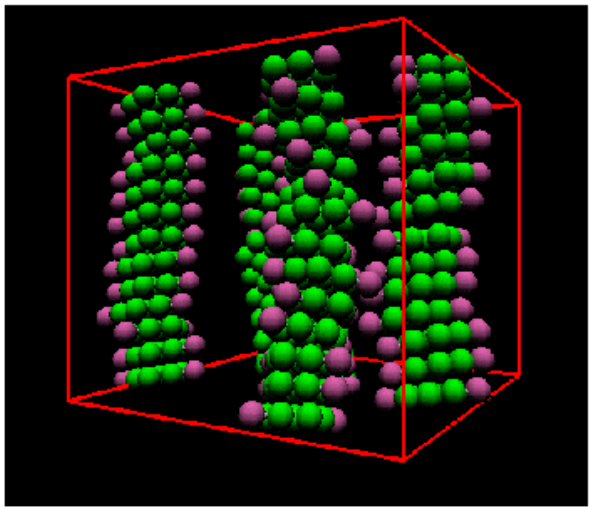

Columnar aggregates with model (a) remain stable over simulation time

Umbrella sampling (Torrie and Valleau 1977)

Umbrella sampling attempts to overcome the sampling problem by modifying the potential function so that the unfavorable states are sampled sufficiently. The modification of the potential can be written as a perturbation and is given by

$$V(r^N) = V_0(r^N) + U(r^N)$$

$U(r^N)$ is the Umbrella potential and could be a function of some order parameter or reaction coordinate

Quite often it is taken to be Quadratic form

$$U(r) = \frac{1}{2} k(r - r_0)^2$$

For configuration that are far from the equilibrium state r0 the Umbrella Potential will be large and so a simulation using the modified potential Will be biased along some relevant reaction coordinate away

Umbrella Sampling

The probability distribution is given by

$$P(r)=\frac{1}{Z}\int dr^{N}\delta[r-r_{0}]\exp[-\beta V(r^{N})]$$

The probability distribution in the presence of Umbrella potential is given by

$$P'(r)=\frac{1}{Z'}\int dr^{N}\delta[r-r_{0}]\exp[-\beta(V(r^{N})+U(r))]$$

$$=\frac{Z}{Z'}\exp[-\beta U(r)]P(r)$$

Thus the original distribution function P(r) can be obtained (to within a multiplicative constant)

$$P(r)=\frac{Z}{Z'}\exp[\beta U(r)]P'(r)$$

The Helmholtz free energy

$$F(r)=-k_{B}T\ln[P(r)]$$

Calculating potential of mean force of two chromonic liquid crystal in water

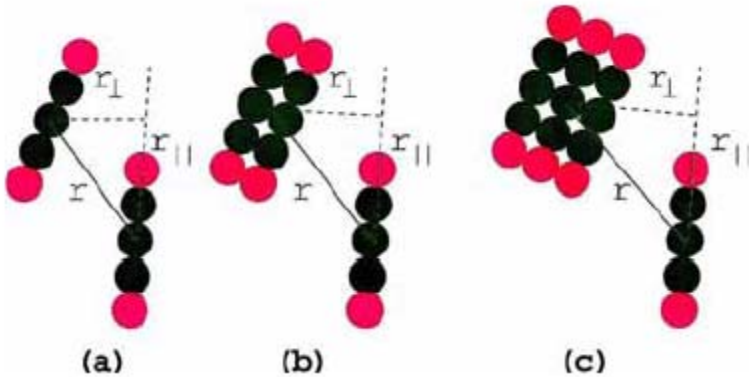

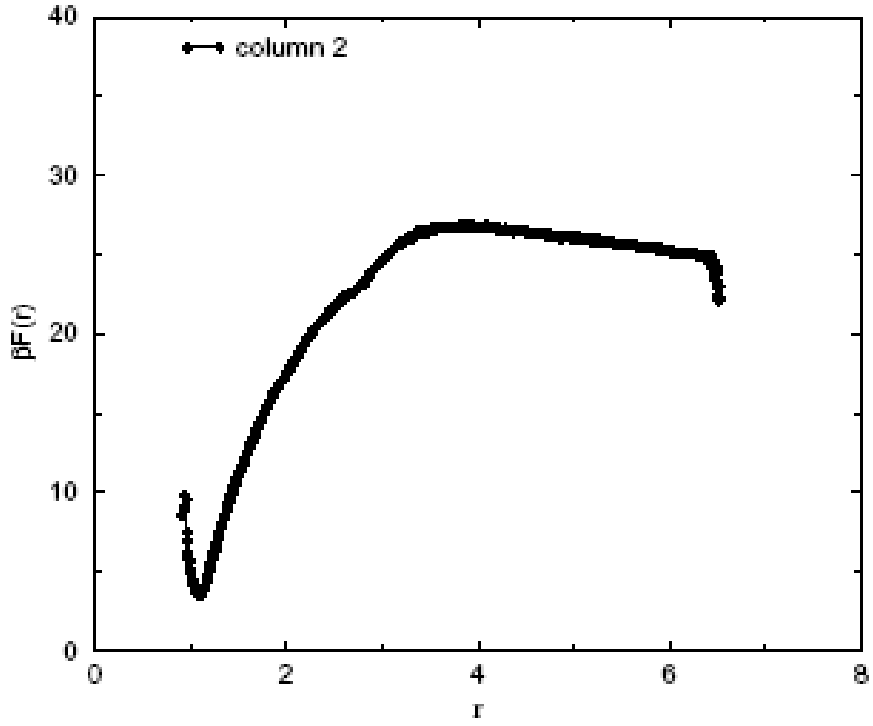

Free energy for larger column (3 and 4)

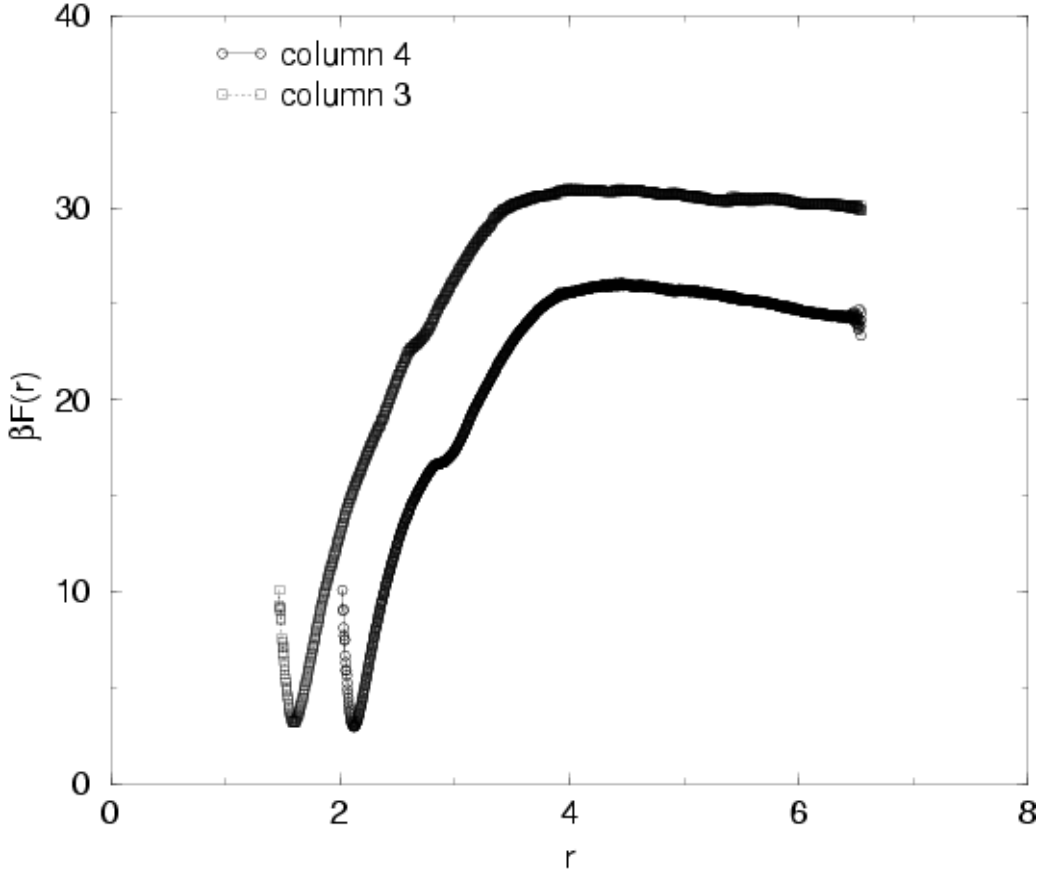

- **Strong attraction at short distance leading face to face chromonic aggregation.**
- **Plateau at larger distance**
- **Increase in free energy at intermediate distance due to respective solvation shells interactions**

By stacking on top of each other the unfavorable hydrophobic interactions with water molecules is reduced and this stacking results in a net increase in the volume available to the water molecules thereby increasing their entropy (depletion force).

Orientation within the column

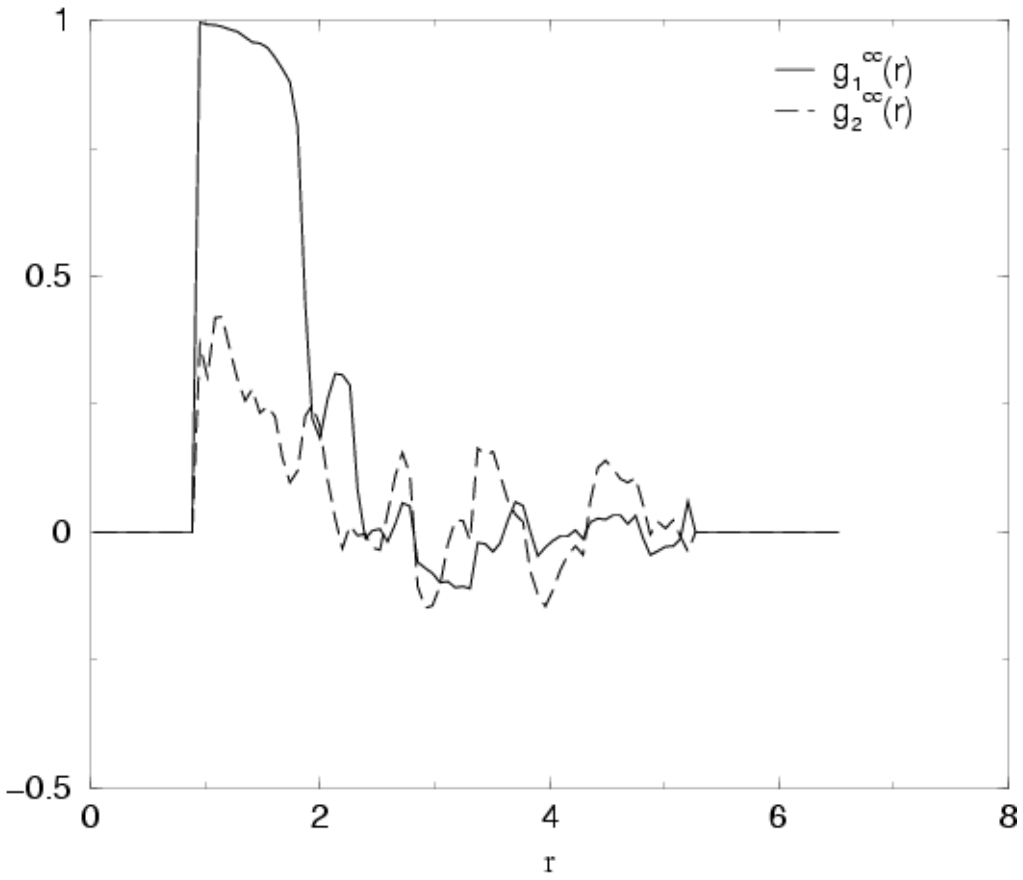

- At the minimum separation (r=1.1σ) the two chromonic are parallel and stacked together (see g1).
- Their in-plane unit vector make an angle to each other as seen from g2.
- With increase in separation they loose their orientation correlations.

Collaborators:

M. A. Glaser

Yves Lansac

N. A. Clark

Kurt Kremer